DESIGN AND ANALYSIS OF BIDIRECTIONAL CHARGERS FOR ELECTRIC VEHICLES

A DISSERTATION

SUBMITTED IN PARTIAL FULFILLMENT OF THE REQUIREMENTS FOR THE AWARD OF THE DEGREE

OF

MASTER OF TECHNOLOGY

In

POWER ELECTRONIC AND SYSTEM

Submitted by

SUYASH PANDEY

(2K22/PES/13)

Under the supervision of

Prof. MADHUSUDAN SINGH

Centre of Excellence for Electric Vehicles and Related Technologies

Electrical Engineering Department

DEPARTMENT OF ELECTRICAL ENGINEERING

DELHI TECHNOLOGICAL UNIVERSITY

(Formerly Delhi College of Engineering)

Bawana Road, Delhi-110042

MAY, 2024

DEPARTMENT OF ELECTRICAL ENGINEERING
DELHI TECHNOLOGICAL UNIVERSITY
(Formerly Delhi College of Engineering)
Bawana Road, Delhi-110042

CANDIDATE'S DECLARATION

I, SUYASH PANDEY, Roll No. 2K22/PES/13 student of M.Tech (Power Electronic and Systems), hereby declare that the project Dissertation titled "**design and analysis of bidirectional chargers for electric vehicles**" which is submitted by me to the Department of Electrical Engineering, Delhi Technological University, Delhi in the partial fulfillment of the requirement for the award of degree ofMasters of Technology, is original and not copied from any source without proper citation. This work has not previously formed the basis for the award of any Degree, Diploma Associateship, fellowship or other similar title or recognition.

Place: Delhi SUYASH PANDEY

Date:

DEPARTMENT OF ELECTRICAL ENGINEERING
DELHI TECHNOLOGICAL UNIVERSITY
(Formerly Delhi College of Engineering)
Bawana Road, Delhi-110042

CERTIFICATE

I hereby certify that the Project Dissertation titled "**Design and analysis of bidirectional chargers for Electric vehicles**" which is submitted by SUYASH PANDEY (2K22/PES/13), Electrical Engineering Department, Delhi Technological University, Delhi in partial fulfilment of the requirement for the award of the degree of Master of Technology, is a record of project work carried out by the student under my supervision. To the best of my knowledge this work has not been submitted in part or full for any Degree or Diploma to this University or elsewhere.

Place: Delhi
Date:

Prof. MADHUSUDAN SINGH
(SUPERVISOR)
Electrical Engineering Department

ACKNOWLEDGEMENT

It is a matter of great pleasure for me to present my dissertation report on "**Design and analysis of bidirectional chargers for Electric vehicles**". First and foremost, I am profoundly grateful to my guide **Prof. Madhusudan Singh**, Department of Electrical Engineering for his expert guidance and continuous encouragement during all stages of this project. His help in form of valuable information and research papers at appropriate time helped in completing this thesis. I feel lucky to get an opportunity to work with him. Not only understanding the subject, but also interpreting the results obtained through simulation study. I am thankful to the kindness and generosity shown by him towards me, as it helped me morally complete the project before actually starting it. I also wish to extend my sincere gratitude to **Dr. Mayank Kumar,** assistant professor DTU for his valuable inputs in completion of this project.

Besides my supervisors, I would also like to thank my seniors for being present during the best and the worst moments of this journey.

I would like to thank **my parents** for their help, encouragement and well wishes during my study at DTU. I dedicate my work to them.

Finally, I like to thank each and every person who were involved directly or indirectly inhelping me to successfully complete this project.

Date:

Place: DELHI SUYASH PANDEY

ABSTRACT

Concerns about climate change and the depleting nature of fossil fuels have attracted attention of researchers toward sustainable development in transportation and rise in popularity of electric vehicles (EVs) in recent years. An essential part of electric vehicles is the battery charging system, which has drawn a lot of research interest, especially when it comes to vehicle-to-grid (V2G) power transfer. Integration of renewable energy and helping the grid to achieve peak load levelling is the main goals of vehicle to grid (V2G). With a specific focus on discussion and analysis of single-phase on-board bidirectional chargers. The design, control, and identification of islanding situations in these chargers are the main research areas. This study includes a thorough analysis of two distinct EV charging systems: one that is based on isolated topology and other based on non-isolated topology. The study involves an improved design methodology that precisely evaluates the damping resistor losses and high-frequency current ripple for both converters. The design, modelling, and simulation of the controllers utilized in the two converters are also included in this thesis. This study focuses on a Modified SEPIC bidirectional charger at both 48V volts and 120V with capacity of 1.1kW and a Dual Active Bridge (DAB) converter with different types of phase shift modulation techniques for optimised output. In this thesis we also talk about Battery, its type, characteristics and design parameters.

TABLE OF CONTENTS

LIST OF FIGURES

LIST OF TABLES

CHAPTER 1

INTRODUCTION

Electric vehicles (EVs) are becoming increasingly practical as the demand for fossil fuels continues to rise. Consequently, a robust and fast charging infrastructure is important for wide acceptability of the electric vehicles in main transportation system. To instill confidence in drivers for long-distance travel, various battery technologies are being proposed, and chargers are being developed in diverse forms and sizes. The charging infrastructure is evolving daily to keep pace with the rapid growth of EVs, ranging from off-board chargers and battery swapping to DC fast charging. The technology behind electric vehicle chargers has advanced significantly, leading to higher energy efficiency and faster charging times.

Modern chargers are equipped with battery monitoring systems that allow for remote access to charging. Some feature cutting-edge vehicle to grid (V2G) technology that can return power to the grid when the vehicle is not in use or parked, thus helping to balance the load demand on the grid.

1.1 Comparison of IC Engine and Electric Vehicle

Both ICE vehicles and EVs offer unique way to approach at leisure transportation, each with its own set of good and bad. ICE vehicles, which has dominated market until recently, operate on the principle of converting chemical energy into mechanical energy through combustion engine. They benefit from a well-established fuel station infrastructure, a wide variety of models, and easily accessible fuel stations. Additionally, ICE vehicles typically offer a higher driving range and require less time to refuel. However, a significant drawback is their substantial contribution in polluting the air and change in climate due to the emission of toxic pollutants and increase in global warming. Further, continuous depletion of petroleum products and their rising prices are major concerns towards use of EVs.

Conversely, EVs are becoming more popularity as a clean, sustainable and reliable alternative, powered by rechargeable batteries and electric motors, resulting in zero tailpipe emissions. This shift leads to better quality in air and reduced reliance on conventional fuels. EVs also provides smooth and quiet driving experience with instant torque and quick acceleration. Although the purchase cost of EVs is relatively high, they tend to be more economical over time compared to ICE vehicles.

1.2 Hybrid Electric Vehicle vs. Electric Vehicle

Although they use different technology in working but the idea is same for the both hybrid EVs and EVs is to lower the emission of harmful gases and making a greener environment. A schematic diagram of EVs and HEVs is shown in Figure 1.1.

All-electric vehicles that run exclusively on electricity are known as electric vehicles, or EVs. They are powered by batteries with recharging capabilities and move by electric motors. Electric cars have nil exhaust emissions, which reduces air pollution and greenhouse gas emissions. This has a major positive ecological impact. However, EVs can be challenging to recharge on lengthy excursions and in areas with a lack of charging stations because they typically have a small driving range and require frequent access to a charging infrastructure. HEVs are made up of an electric motor, battery system, and IC engines. Minimizing emissions and maximizing fuel efficiency are the two main objectives of HEV design.

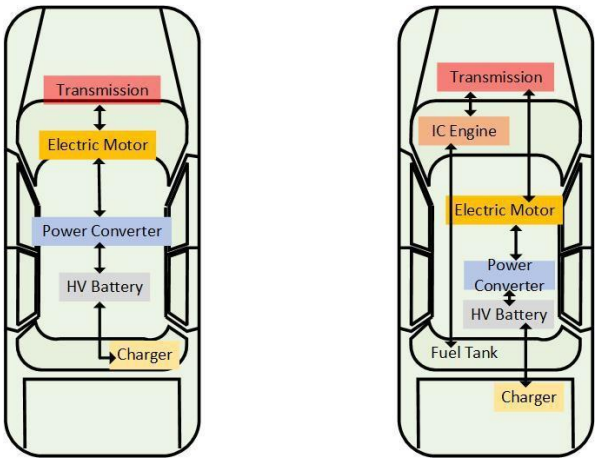

Figure 1.1: Schematic diagram of BEVs and HEVs

When more power is needed or at higher speeds, the internal combustion engine powers the vehicle, while the motor helps with low-speed driving and initial acceleration. Compared to conventional cars, hybrid electric vehicles (HEVs) produce less pollution and use less gasoline because they may operate entirely on electricity in certain situations. They also remove the limit on the range pertaining to fully EVs as the internal combustion engine picks up when the battery is depleted. However, as hybrid electric cars (HEVs) still run mostly on fossil fuels, their ability to cut emissions may be limited compared to fully electric cars.

1.3 Chargers for electric vehicle battery

Chargers for EV battery are essential to facilitate the easy and effective recharging of electric vehicles as the world accepts the shift to modern transportation. These chargers which offer a dependable and convenient way to recharge the vehicle's battery, are crucial aspects for electric vehicles' infrastructure. To meet the varied needs of owners of electric vehicles, EV battery chargers are available in a variety of shapes and charging capacities. In their most basic form,

Level 1 chargers fit into a typical household outlet and are intended for residential use. These generally work at 230V 16A and can be connected to wall socket to charge the EVs .Despite having the slowest charging rate, Level 1 chargers are a practical choice for charging overnight, guaranteeing that the car is prepared for everyday use. Adds approximately 50 to 80 km of range when charging for 10hrs.

Level 2 chargers are basically private and charging stations for the general public to provide faster charging. These chargers work at higher power levels and require a dedicated charging unit generally working at 240V 80A. This allows them to dramatically reduce charging times. For regular charging demands, level 2 chargers are the perfect answer because they enable PEV owners to quickly refuel their cars. Adds approximately 65 to 100 km of range when charging for 10hrs.

Level 3 These are the fastest chargers using DC power and are available at public charging stations for even faster and more convenient charging. Direct current (DC) is used by DC fast chargers to quickly charge the car's battery. Working at about 50kW and delivering power to the battery and charging it in from 30 mins to 1 hr. Adds approximately 160 to 320 km of range when charging for 1hrs.

The recharging of battery is necessary in order to start and extrat energy from the battery and operate on its full capability. Battery charger's power density, charging time, sustainability, and efficiency are crucial components that set it apart from the competition. These device characteristics are influenced by the controller, switching mechanisms, and component choice. Microcontrollers are used to implement digital control techniques. Figure:- 1.2 displays about the overall architectural block diagram of a charger.

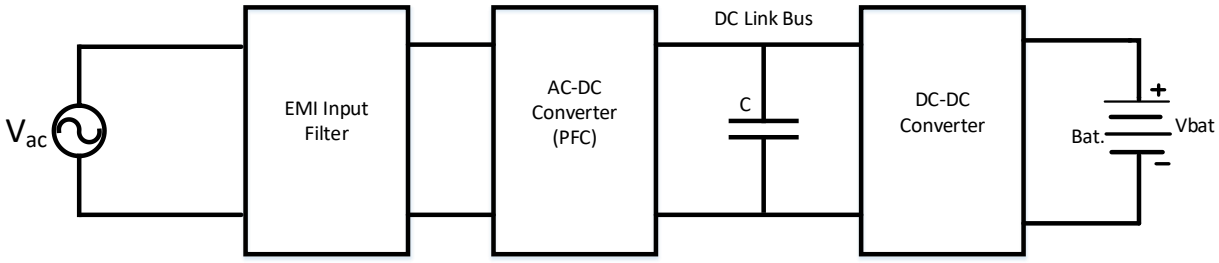

Figure 1.2: Topology of Charger Circuit

1.4 Battery Technology

Selecting a particular type of battery for our Electric vehicles is a very crucial task as generally battery costs the half of the whole vehicle itself hence to make the vehicles more effectively priced in the market and for what purpose the vehicle will be used, the battery selection should be taken into consideration with utmost importance.

In selecting a battery there are some requirements that must be fulfilled for example energy and power, energy density, operating temperature, self-discharging rate, number of the life cycle , cost, efficiency and environmental adaption. Keeping these parameters into mind battery can be divided into 4 categories:

- **i** Lithium-ion Battery
- **ii** Lead-acid Battery
- **iii** Nickel-Metal Hydride Battery
- **iv** Ultra capacitors

1.4.1 Lithium-Ion battery

Lithium-Ion battery have become industry standard in rechargeable batteries technology Because of their lengthy life cycle, high energy density, and lightweight design. These batteries have their cathode made of lithium cobalt oxide or lithium iron phosphate[2] or other lithium compounds the anode is usually made of graphite electrolyte[2] is generally a lithium salt dissolved in organic solvent, a separator which is micro-porous membrane is used which prevents the direct contact between anode and cathode.

Lithium-ion has several advantages such as greater energy density providing high energy per unit weight and volume. Low self-discharge rate longer charge cycle .But there are some disadvantage of using lithium ion battery such as thermal runaway, limited amount of lithium and cobalt deposits in the world causing the lithium battery to be more costly

than others

1.4.2 Lead Acid battery

These are the oldest technologies present in reachable batteries and are mainly used in automotive and industries due to their reliability and less buying cost. In their design the cathode is made up of lead dioxide and anode is made up of sponge lead and electrolyte is made of dilute sulphuric acid [3]. Reasonably priced to manufacture and acquire, reliable technology has a long history of use. Because they can provide large surge currents, they are appropriate for applications involving engine starting. Some disadvantages are, heavier and more voluminous than contemporary Li-ion batteries. Shorter lifespan in terms of cycles of charging and discharging. Some kinds need to have their electrolyte levels checked on a regular basis. Recycling lead can be dangerous because it is poisonous. These batteries are generally used in car batteries, renewable systems, off grid backup power systems.

1.4.3 Nickel-Metal Hydride (NiMH) battery

NiMH battery is a famous kind of rechargeable battery found in hybrid cars and consumer devices. They stand on a middle ground between lead-acid battery durability and Li-ion battery high density of energy. The battery construction is as follows: the cathode is made up of Nickel oxyhydroxide , anode is made of Hydrogen- absorbing alloy and electrolyte present is potassium hydroxide. Advantage of NiMH battery is that higher energy capacity in comparison to batteries made of nickel-cadmium (NiCd) less harmful metals are present than in lead-acid and nickel-cadmium batteries. Rechargeable several times. However they suffer from faster rate of self-discharge than Li-ion batteries. May have decreased capacity (albeit less severe than in NiCd batteries) if not completely depleted before recharging and more costly than batteries made of lead acid. These batteries can be used in AA and AAA batteries, cordless power drills and other portable devices.

1.5 Ultracapacitors or Supercapacitors

Supercapacitors, another name for ultracapacitors, are energy-storage devices that rely less on chemical reactions and more on electrostatic forces. In comparison to normal batteries hey have quick charge/discharge times and have very high power density. The electrodes are made up of activated carbon or high surface area material and electrolyte is taken such that it has adequate ion conductivity and the separator is material that allows

ions to pass through it without allowing electrical conductivity between the electrodes.They are very efficient with minimal energy loss during charging or discharging cycle. Quickly delivers and absorbs high currents; operates well throughout a wide temperature range; may be charged and discharged in a matter of seconds; and can be cycled for hundreds of thousands to millions of times without experiencing significant deterioration .The main disadvantage is that compared to batteries, it holds less energy per unit weight or volume. More expensive per watt-hour than batteries. These ultracapacitors can be used in short term backup power, providing burst of power in electrical and mechanical system, can help with the levelling of voltage fluctuations.

1.6 Modelling of Battery

Figure 1.3 shows the analogous circuit model, which is a typical electrical representation of a lithium-ion battery. This model makes up of multiple circuit components that simulate how a Li-ion battery would act in various scenarios. Here is an illustration of a basic electrical circuit model:

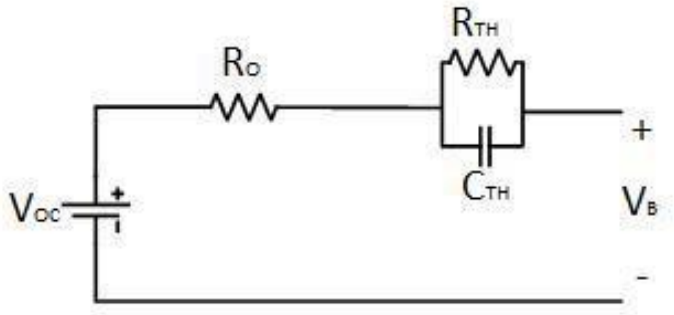

Figure 1.3:- Equivalent circuit of Li-Ion Battery

1.6.1 Open-Circuit Voltage (V_{OC}):

This is the battery's voltage in the absence of any current. State of charge (SoC) of the battery plays a major role and is often ascertained by measurement or calibration.

1.6.2 Internal Resistance (R_{th}):

The internal resistance present in the battery is what prevents current from flowing through it. It encompasses a range of resistance sources, including contact resistance, electrode resistance, and electrolyte resistance. Within the battery, internal resistance results in power losses and voltage drops. The internal resistance in this model is explained by both the polarization resistance (RTH) and the ohmic resistance (Ro).

1.6.3 Internal Capacitance (C_{th}):

The battery's capacity to hold and release charge is represented by capacitance. It explains the intercalation capacitance and the double-layer capacitance at the electrode-electrolyte interface.

1.6.4 Operating voltage of the Battery (V_B):

It indicates operating voltage of battery that is battery is connected to a source or acting as as source.

1.7 Charging and Discharging Characteristics of Battery

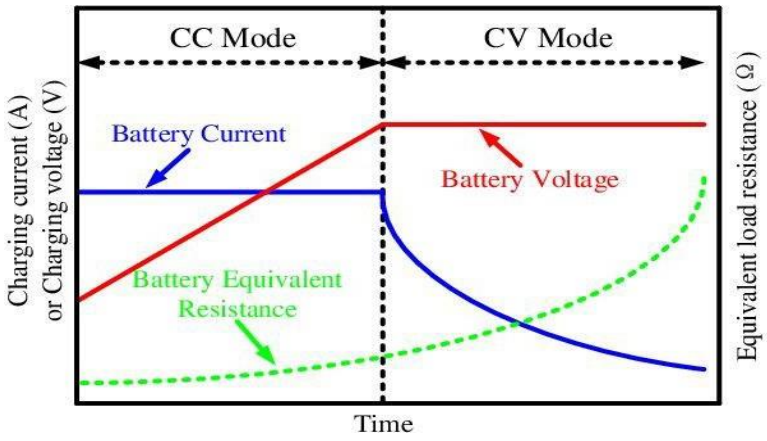

Figure-1.4: Characteristics of the cell

When charging Li-ion batteries, the constant current and constant voltage (CC and CV) mode is often used. The performance of a single lithium-ion cell in charging at a specified voltage (V_{DC}) of a cell is shown in Figure 1.4. The charging process can be divided into four noteworthy stages [5]. The turning point denotes the switch from the CC to CV charging mode and the rated value indicates when the battery acquires a stable state. When the cell is exhausted, the voltage falls below its nominal rating. The battery is first charged using a constant current operation until it reaches the kink point, at which point its voltage must be increased to its nominal value and is at a 100% state of charge (SoC). Hence the charging of battery is done in constant voltage until the charging current falls to an appropriate level.

The efficiency and durability of electric vehicles (EVs) and other battery-powered devices are highly dependent on battery health. You can tell if a battery is healthy by looking at these important metrics:

1.7.1 State of Charge (SoC):

It is defined as its present charge level as a percentage of its maximum capacity. It helps customers plan charging and usage by indicating the amount of energy left in the battery. To avoid damaging the battery, accurate system-of-charge monitoring is necessary to avoid overcharging or deep draining.

1.7.2 State of Health (SoH):

SoH is a measure of the battery's overall condition relative to its initial condition upon purchase. The standard unit of measurement is the percentage, with 100% indicating the initial capacity and performance of the battery. Charge cycles, temperature fluctuations, and aging are some of the processes that cause SoH to decrease with time. Capacity and efficiency are both diminished with a decreased SoH.

1.7.3 State of Power (SoP):

SoP is a measure of a battery's maximum power output that can be displayed at any given moment. The internal resistance of the battery, temperature, and current state of charge are some of the variables that affect it. The SoP can be negatively impacted by low temperatures or high internal resistance, which in turn affects the device's performance.

1.7.4 Energy Storage Capacity:

Measured in ampere-hours (Ah) or watt-hours (Wh), a battery's capacity is the overall quantity of energy it can store. The quantity of energy that a battery can store and release decreases as its capacity deteriorates over time as a result of being charged and discharged multiple times.

1.7.5 Resistance from Within:

The barrier to current flow within the battery is known as internal resistance. Greater heat generation and energy loss might result from higher internal resistance, which in turn reduces efficiency and performance. It worsens the battery's capacity to swiftly supply power as it ages and is used more frequently.

1.7.6 Cycle Life:

The cycle life of a battery is the amount of times it can be fully charged and discharged before losing some proportion of its initial capacity, usually about 80%. While significant discharges can reduce a battery's cycle life, a longer cycle life implies a more robust battery.

1.7.7 Battery Temperature:

Battery performance and lifespan are greatly impacted by temperature. Batteries are susceptible to degradation, decreased efficiency, and accelerated aging when exposed to extremely hot or cold temperatures. Optimal battery health is achieved by proper temperature management.

1.7.8 Battery Voltage:

Both the system on a chip (SoC) and the load on the battery affect its voltage. It is possible to estimate SoC and make sure the battery is operating within safe limits by monitoring the voltage. Both low voltage and high voltage can shorten the life of a battery.

1.7.9 Rates of Charging and Discharging:

Charge and discharge rates, abbreviated as C-rates, have an effect on the life of a battery. An increase in stress, which in turn increases heat and speeds up degradation, can be caused by high C-rates. To keep batteries in good condition, it's best to charge and discharge them at moderate rates.

1.7.10 The rate of self-discharge:

When a battery is not being used, its charge slowly drains away, a process known as self-discharge. The condition or quality of the battery may be compromised if its self-discharge rate is excessively high. It changes as the battery ages and the temperature changes. The health, safety, and longevity of batteries in a variety of applications—and EVs in particular—can be better managed with an understanding of and adherence to these principles. The performance and lifespan of your battery can be greatly improved with regular maintenance and following recommended usage guidelines.

1.8 Literature Review

S. S. Williamson et.al. [1]: (2013): ("Strategies for managing energy in electric and plug-in hybrid electric vehicles"). Energy management in electric vehicles and plug-in hybrid electric vehicles is the subject of this book, which aims to improve both efficiency and performance.

A. Emadi et.al. [2]: (2008): "Power Electronics and Motor Drives in Electric, Hybrid Electric, and Plug-In Hybrid Electric Vehicles," published in "IEEE Transactions on Industrial Electronics." The role of motor drives and power electronics in the operation and efficiency of PHEVs, HEVs, and EVs is examined in this study.

M. Yilmaz et.al. [3] (2012): "Review of charging power levels and infrastructure for plug-in electric and hybrid vehicles," given at the "IEEE International Electric Vehicle Conference (IEVC)". In order to accommodate the increasing number of plug-in and hybrid vehicles, this review article investigates various charging power levels and the necessary infrastructure.

Kavuri Poornesh et.al. [4] (2020): "A Comparative Study on Electric Vehicles and Internal Combustion Engine Vehicles," the paper was given at the "International Conference on Smart Electronics and Communication (ICOSEC)". This study examines the pros and cons of electric and internal combustion engine automobiles side by side.

H. Wang et.al. [5] (2014): "Design and analysis of a full-bridge LLC-based PEV charger optimized for wide battery voltage range," published in "IEEE Transactions on Vehicular Technology." The design of a plug-in electric car charger based on a full-bridge LLC is the main subject of this study.

Huishuang Fan et.al. [6] (2019): "Output voltage ripple reduction control strategy for three-phase combined PFC converter under grid voltage unbalance," given at the "22nd International Conference on Electrical Machines and Systems (ICEMS)". In the context of an imbalanced grid, this study discusses methods for lowering the output voltage ripple

of PFC converters.

Rafael Pena-Alzola et.al. [7] (2016): "Control Design of a PFC with Harmonic Mitigation Function for Small Hybrid AC/DC Buildings," published in "IEEE Transactions on Power Electronics." A power factor correction converter with harmonic mitigation functions is described in this paper's control design.

J. Gupta et.al. [8] (2022): "A Single Stage Bridgeless Isolated AC-DC Conversion System for Light Electric Vehicles Charging Application," appeared in the IEEE Transactions on Transportation Electrification. A lightweight electric vehicle (LEV) AC-DC conversion system with a single stage and no bridges is the subject of this early access article.

Jinming Xu et.al. [9] (2021): "Overview of SOGI-Based Single-Phase Phase-Locked Loops for Grid Synchronization Under Complex Grid Conditions," in the IEEE Access journal. Using a second-order generalized integrator (SOGI) as its foundation, this work examines single-phase phase-locked loop systems that synchronize with the grid.

B. Whitaker et.al. [10] (2014): "A high-density, high-efficiency, isolated on-board vehicle battery charger utilizing silicon carbide power devices," featured in the IEEE Transactions on Power Electronics. This study focuses on a silicon carbide power device on-board vehicle battery charger that is very efficient.

A. Bocca et.al. [11] (2020): "Optimal Life-Cycle Costs of Batteries for Different Electric Cars," delivered at the AEIT International Conference of Electrical and Electronic Technologies for Automotive (2013). The research delves into the cost-life analysis of electric car batteries.

T. Konjedic et.al. [12] (2015): "DCM-based Zero-Voltage Switching Control of a Bidirectional DC-DC Converter With Variable Switching Frequency," published in the

IEEE Transactions on Power Electronics. The regulation of zero-voltage switching in bidirectional DC-DC converters is the subject of this investigation.

A. V. Mirtchev et.al. [13] (2022): "Design Methodology Based on Dual Control of a Resonant Dual Active Bridge Converter for Electric Vehicle Battery Charging," published in the IEEE Transactions on Vehicular Technology. A resonant dual active bridge converter is designed for electric vehicle battery charging in this research.

B. K. Padhi et.al. [14] (2016): "Controller design for reduced order model of SEPIC converter," delivered at the International Conference on Signal Processing, Communication, Power, and Embedded Systems in the title of the paper. This study details the development of a SEPIC converter controller for a lower-order model.

F. Jauch et.al. [15] (2014): "Generalized modeling and optimization of a bidirectional dual active bridge DC-DC converter including frequency variation," the paper was presented at the International Power Electronics Conference (IPEC-Hiroshima - ECCE ASIA). In this work, we model and optimize a DC-DC converter that uses a bidirectional dual active bridge.

D. Committee et.al. [16] (2014): "IEEE Recommended Practice and Requirements for Harmonic Control in Electric Power Systems," a publication by the IEEE Power and Energy Society. Harmonic control in electrical power systems is described in this paper.

R. W. Erickson et.al. [17] (2007): Springer Science & Business Media's Essentials of Power Electronics. One can get a thorough grounding in the principles of power electronics from this textbook.

Pratap Ranjan Mohanty et.al. [18] (2015): "An Active PFC Boost Converter Topology for Power Factor Correction," delivered at the Annual IEEE India Conference and Exhibition (INDICON). A power factor correction boost converter topology is presented

in this work.

Rahul Pandey et.al. [19] (2018): "A Power Factor Corrected Electric Vehicle Battery Charger Using Boost Converter," delivered at the IEEE India International Conference on Power Electronics (IICPE). A boost converter-based power factor corrected electric vehicle battery charger is the subject of this article.

João Paulo et.al. [20] (2010): "A Review of Single-Phase PFC Topologies Based on The Boost Converter," delivered at the IEEE/IAS proceedings. Several boost converter-based single-phase power factor correction topologies are reviewed in this article.

Murat Yilmaz et.al. [21] (2013): "Review of Battery Charger Topologies, Charging Power Levels, and Infrastructure for Plug-In Electric and Hybrid Vehicles," a paper published in the IEEE Transactions on Power Electronics. This all-inclusive guide discusses the essential infrastructure for electric and hybrid vehicles, as well as various battery charger topologies and power levels.

Wenjin Dai et.al. [22] (2008): "Design of Single Phase Boost-PFC Converter With Fast Voltage Regulator," shown at the IEEE International Conference on Industrial Technology. This paper describes the design of a rapid voltage regulator single-phase boost PFC converter.

V. Randive et.al. [23] (2020): "Simplified State-Space Average Model and Control Strategy for the Dual Active Bridge Power Converter," lectured at the IEEE Power India International Conference (PIICON). A dual active bridge power converter's simplified state-space model and control method are presented in this research.

Senthilkumar et.al. [24] (2018): "Fractional Order Controller Design for SEPIC Converter Using Metaheuristic Algorithm" . In this study, we look at how to use a metaheuristic method to build a fractional-order controller for a SEPIC converter.

S. Choudhury et.al. [25] (2003): "Average current mode controlled power factor correction converter using TMS320LF2407A," reads the application note from Texas Instruments. Using the TMS320LF2407A microcontroller, this document explains how to build an average current mode driven PFC converter.

H. Plesko et.al. [26] (2008): "Creative ideas for combining the electric motor and supplementary direct current converter in hybrid cars," published in the IEEE Transactions on Power Electronics. In this article, we take a look at several novel ideas for hybrid electric drives that incorporate auxiliary DC-DC converters.

S. Kim et.al. [27] (2015): "Multifunctional onboard battery charger for plug-in electric vehicles," published in the IEEE Transactions on Industrial Electronics. The focus of this study is a plug-in electric vehicle (PHV) onboard battery charger with multiple uses.

M. A. Khan et.al. [28] (2014): "A Bi-directional DC-DC Converter with Overlapping Input and Output Voltage Ranges and Vehicle to Grid Energy Transfer Capability," presented at a conference organized by IEEE. The purpose of this study is to talk about a DC-DC converter that can transmit energy from vehicles to the grid in both directions.

R. Teodorescu et.al. [29] (2011): Renewable Energy Systems: Grid Converters for Solar and Wind Power, published by John Wiley & Sons. The book delves deeply into the topic of grid converters as they pertain to renewable energy sources.

H. Guan-Chyun et.al. [30] (1996): methods utilizing phase-locked loops? It was published in the IEEE Transactions on Industrial Electronics as a questionnaire. Various phase-locked loop approaches utilized in industrial electronics are reviewed in this survey article.

M. Karimi-Ghartemani et.al. [31] (2001): "A new phase-locked loop (PLL) system," announced at the IEEE Midwest Symposium on Circuits and Systems (MWSCAS). The

article presents a novel power network PLL system.

S. Golestan et.al. [32] (2012): "Design and Tuning of a Modified Power-Based PLL for Single-Phase Grid-Connected Power Conditioning Systems," published in the IEEE Transactions on Power Electronics. A modified power-based PLL for grid-connected systems is designed and tuned in this work.

A. Ozdemir et.al. [33] (2013): "A software-based digital phase-locked loop for power electronics applications: fast and robust," published in the International Electrotechnical Transactions, Generation, Transmission & Distribution journal. A digital PLL for power electronics that is software-based is presented in this paper.

A. Ohori et.al. [34] (2014): "Phase-Locked Loop Using Complex-Coefficient Filters for Grid-Connected Inverter," published in the Japanese journal Of Electrical Engineering. For inverters that are connected to the grid, this research delves into a PLL that makes use of complex-coefficient filters.

M. M. Begovic et.al. [35] (1993): "Frequency tracking in power networks in the presence of harmonics," published in IEEE Transactions on Power Delivery. This research focuses on frequency tracking in power networks with harmonic distortion.

D. Nedeljkovic et.al. [36] (1999): "Reference to the network for synchronization of active power filters' currents," published in the IEEE Transactions on Industrial Electronics. Active power filters and grid synchronization is the topic of this article.

R. Weidenbrug et.al. [37] (1993): "New synchronization method for thyristor power converters to weak AC-systems," published in the IEEE Transactions on Industrial Electronics.. A novel technique for thyristor power converter synchronization is introduced in this study.

R. W. Wall et.al. [38] (2003): "Simple methods for detecting zero crossing," delivered at the IEEE Industrial Electronics Society Annual Conference (IECON). In this paper, we will go over some basic techniques for detecting zero crossings in power electronics.

P. Rodriguez et.al. [39] (2006): "Advanced Grid Synchronization System for Power Converters under Unbalanced and Distorted Operating Conditions," delivered at the IEEE Industrial Electronics Conference (IECON). A state-of-the-art power converter grid synchronization system is presented in this study.

Gardner, F. M. et.al. [40] (1966): Phaselock Techniques, written by John Wiley and Sons and published by HP. Methods for achieving phase-locking in electrical systems are discussed in this book.

Utsav Sharma et.al. [41] (2020): "An Onboard Charger for Light Electric Vehicles," delivered at the IEEE International Conference on Power Electronics, Drives and Energy Systems (PEDES). A lightweight electric vehicle's onboard charger is the subject of this paper's design.

Ionel "Dan" Jitaru et.al. [42] (2012): "A High Efficiency 2KW DC-DC Converter for Automotive Application," that was presented at the IEEE Applied Power Electronics Conference and Exposition (APEC). An efficient DC-DC converter designed for use in automobiles is introduced in this work.

Chan-Song Lee et.al. [43] (2011): "Research on 1.5 kW Battery Chargers for Neighborhood Electric Vehicles," lectured at the IEEE Conference on Vehicle Power and Propulsion. Local electric vehicle (EV) battery chargers are the subject of this study.

Dingsihao Lyu et.al. [44] (2021): "Impacts of Different Charging Strategies on the Electric Vehicle Battery Charger Circuit Using Phase-Shift Full-Bridge Converter," lectured at the IEEE International Power Electronics and Motion Control Conference

(PEMC). The effects of different charging procedures on electric vehicle battery chargers are investigated in this study.

Mohd Shahnawaz Khan et.al. [45] (2020): "Design of On-Board Battery Charger using Interleaved Bridgeless Type PFC and Phase Shifted Full Bridge Converter," lectured at the IEEE International Students' Conference on Electrical, Electronics and Computer Science. Using a phase-shifted full-bridge converter and interleaved bridgeless PFC, this paper details the design of an onboard battery charger.

1.9 Objectives of the Present Work

Objective of this thesis is to design and analyze EV chargers, one isolated and other non-isolated topology in order to implement them in low powered electric vehicles. This thesis also explains the design of both of the chargers and the control mechanism related to it. A brief summary of the work is as follows.

i For non-isolated charger the topology used is a Modified version of the traditional SEPIC converter is taken into consideration. The SEPIC converter is modified by using switched capacitance circuit and using 3 switches to incorporate bidirectional functionality, the use of switched capacitance ensures that the converter's component size is decreased and hence decreasing the cost.

ii For isolated charger, the topology that is studied is Dual Active Bridge (DAB) converter. The DAB converter uses a transformer and a primary side bridge and a secondary side bridge which then uses phase shift techniques to transfer power from primary side to secondary side, the phase shift technique being used here is single phase shift (SPS) technique.

iii All the design calculations of both Modified SEPIC and DAB are done in a single chapter along with the matlab simulations, the simulation shows waveforms of respective voltages, currents, ripples in them voltage stress present in the switches and components.

1.10 Outline of Thesis:

Chapter 1:- In this chapter, a comprehensive overview to Electric Vehicles and their technology giving information on the importance of a feedback structure. It also tells about the charging levels and battery charging characteristics

Chapter 2:- A Bidirectional Charger topology has been explained in the chapter. The Modified-SEPIC DC-DC converter being used for low powered EVs with switched capacitance inclusion to decrease the size of component use and better control strategy for both G2V and V2G power flow.

Chapter 3:- This chapter considers the design of Dual Active Bridge converter working in single phase shift (SPS) mode

Chapter 4:- This chapter presents the design and mathematical calculations and matlab Simulink simulation results.

Chapter 5:- This chapter, the main contribution in the thesis are summarised. Also this thesis highlights the possibility for further study opportunities and summarizes the contributions made by this thesis.

1.11 Conclusion

This thesis begins with an overview of the key differences between internal combustion engines (ICEs) and electric vehicles (EVs) in Chapter 1. Moreover, a succinct description of electric vehicles (EVs) and hybrid electric vehicles (HEVs).

The progress in electric vehicles (EVs) and hybrid electric vehicles (HEVs) has resulted in the acceptance of high voltage Lithium-Ion battery packs for fuel. The potential benefits of using Li-ion batteries also understanding charging profile referred to as constant current and constant voltage mode, as advocated by battery makers. Moreover, an exhaustive elucidation of the battery's comparable electrical model is described. The literature review also categorises EV chargers according to their power levels and further subdivides into power requirements and availability. The section additionally examines previous research on EV chargers and their corresponding converters. The EV charger layout includes a Basic Block diagram is made of a PFC unit as a front end converter with a suitable rating DC-DC converter as a backend converter.

CHAPTER 2

MODIFIED SEPIC CONVERTER FOR LIGHT-WEIGHT EVS

2.1 Introduction

In this Chapter a study about traditional SEPIC converter and modified-SEPIC is presented. The modifications ensure the converter to run in bidirectional mode providing both Forward power flow and reverse power flow operations. The modifications ensures the component size is decreased and this is achieved with the help of introduction of switched capacitance into traditional SEPIC topology. This topology works in four mode of operation two of them are there for forward mode and two for reverse mode.

2.2 Circuit description

Figure 2.1 shows the traditional SEPIC converter with two inductors and two capacitors along with one switch and diode. To decrease the size of the capacitors and inductors and make it bidirectional in nature we do the modifications by using switched capacitance for C_1 and using three switches which helps in bidirectional working.

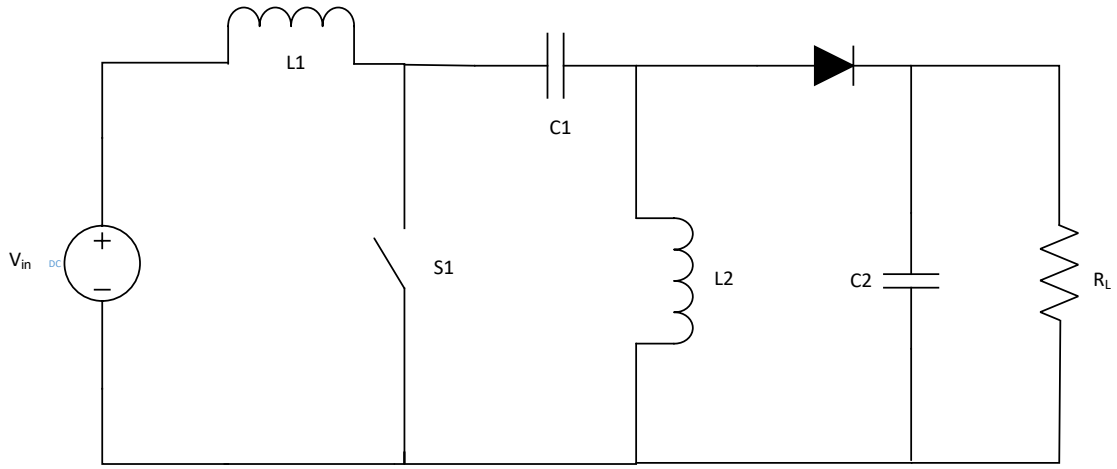

Figure 2.1: Traditional SEPIC converter

Figure 2.2 shows modified-SEPIC which is modified by using Switched capacitance C1and C2 and three switches Q1, Q2, Q3.

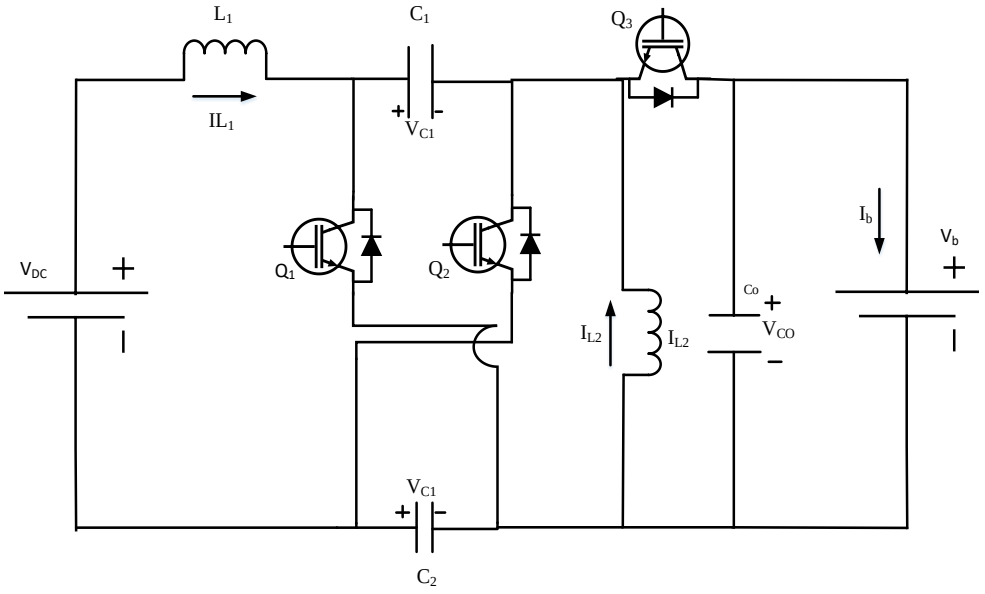

Figure 2.2: Proposed Modified SEPIC charger topology

The battery charger is designed to function in CCM mode, which is significant. The modified-SEPIC converter's circuit diagram is shown in following figure to show different modes in forward and reverse power flow.

2.2.1 Circuit Analysis

(a) Working In Forward Power Flow

In this mode the converter works in buck mode delivering power to the battery from the source voltage using switches Q1 and Q2 and Q3 is used as bypass diode.

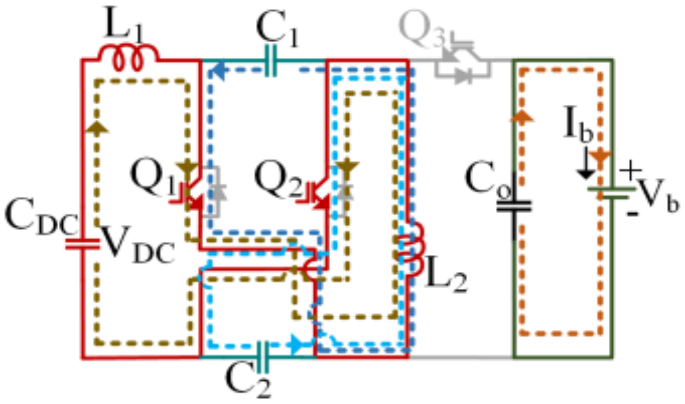

Figure 2.3 mode I circuit in forward mode

Mode I : In this mode switch Q1 and Q2 "ON". The capacitors which are C1 and C2 are

discharged charging the battery and the inductors L1, L2, and L2 are charged as shown in Figure 2.3.

$$v_{L1} + v_{L2} = V_{DC} \tag{2.1}$$

$$v_{L2} = v_{C1} \tag{2.2}$$

$$v_{L2} = v_{C2} \tag{2.3}$$

$$v_{Co} = v_b \tag{2.4}$$

$$i_{L2} = i_{C2} + i_{L1} + i_{C1} \tag{2.5}$$

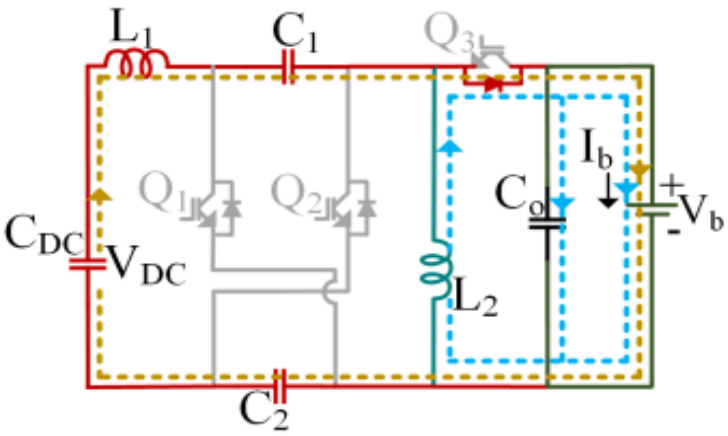

Figure 2.4 mode II circuit in forward mode

Mode II : In this mode switches Q1 and Q2 are switched "OFF". The inductor L1 discharges through the C1, battery, and C2 during this process. In addition, the battery receives its stored energy from the discharge of the inductor L2 as shown in Figure 2.4.

$$v_{L1} + v_{C1} + v_{Co} + v_{C2} = V_{DC} \tag{2.6}$$

$$v_{L2} = -v_{Co} \tag{2.7}$$

$$v_{Co} = v_b \tag{2.8}$$

$$i_{C1} = i_{C2} = i_{L1} \tag{2.9}$$

The relation between duty ratio and source voltage and battery voltage is as follows:

$$M = \frac{V_b}{V_{DC}} = \frac{D}{2(1-D)} \tag{2.10}$$

(b) Working In Reverse Power Flow

During Reverse mode operation, the current flows from battery to the source and hence

the power flow is being reversed, this is done by using switch Q3.

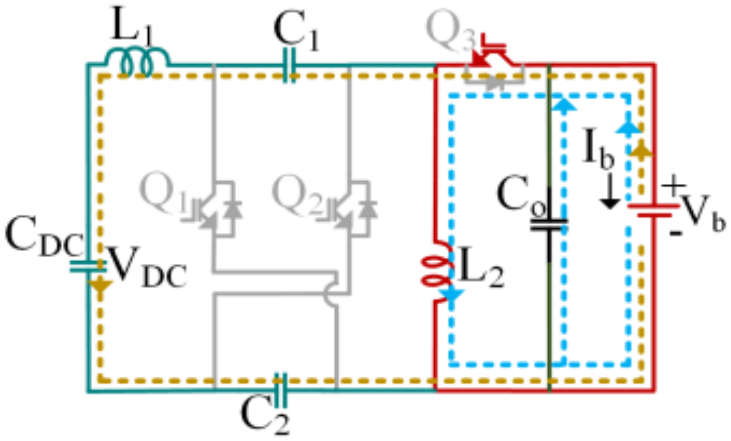

Figure 2.5 : mode I operation of converter in reverse mode

Mode I : In this mode switch Q3 operates and turns on. L2 and L1 inductors begin to charge which in turn increases inductor currents. Furthermore, the source receives the necessary power from the capacitors C1 and C2 as shown in Figure 2.5.

$$v_{L1} + v_{C1} + v_{Co} + v_{C2} = V_{DC} \tag{2.11}$$

$$v_{L2} = -v_{Co} \tag{2.12}$$

$$v_{Co} = v_b \tag{2.13}$$

$$i_{C1} = i_{C2} = i_{L1} = i_{L2} \tag{2.14}$$

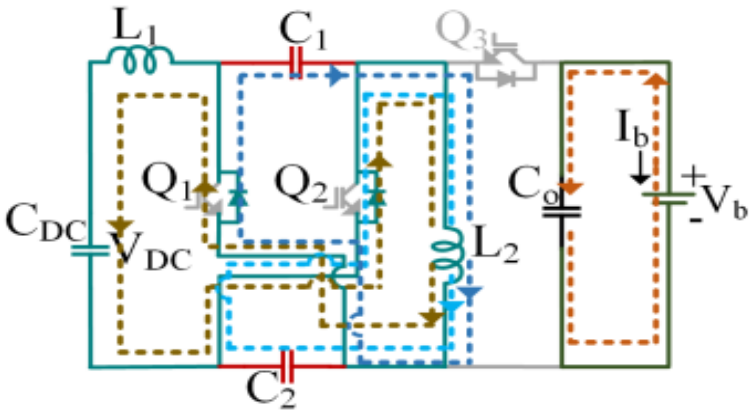

Figure 2.6 : mode II operation of converter in reverse mode

Mode II : In this mode Q3 turns "OFF". The Source receives power from stored energy in inductors L1 and L2 by discharging them and using its energy to charge the capacitors C1 and C2 as shown in Figure 2.6.

$$v_{Co} = v_b \tag{2.15}$$

$$v_{L1} + v_{L2} = V_{DC} \tag{2.16}$$

$$v_{C1} = v_{C2} = v_{L2} \tag{2.17}$$

$$i_{C1} + i_{C2} + i_{L1} = i_{L2} \tag{2.18}$$

The volt-second balanced technique across the inductor L2, determines the voltage transformation of the converter and duty ratio for the same.

$$M' = \frac{V_{DC}}{V_B} = \frac{D'}{2(1-D')} \tag{2.19}$$

Thus from equation (10) and (19),

$$D' = 1 - D \tag{2.20}$$

2.3 Switched Capacitance

Power converters made entirely of switches and capacitors have been in use for a while and are commonly used in diode-capacitor voltage multipliers [1-4].The recent attention on the use of switched capacitance in multiplying the voltage in dc-dc converters, as shown in Figures 2.7 and 2.8, is noteworthy.

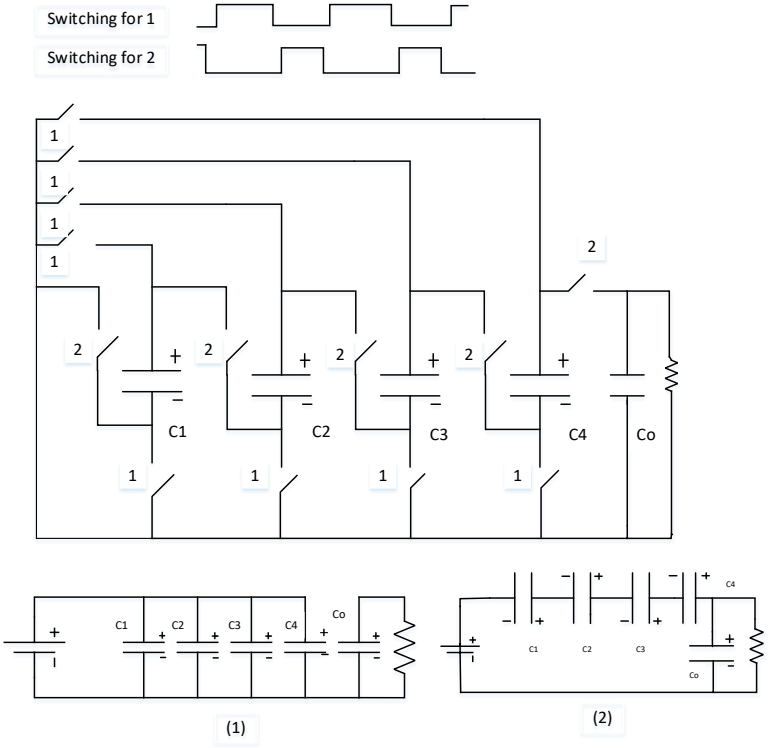

Figure 2.7 : A Switched Capacitor converter with 5 capacitors.
Step up conversion ratio $M=V_o/V_g=5$.

Switched Capacitance (SC) DC-DC converters offer numerous advantages over traditional power converters that utilize both inductive and capacitive energy storage. They are particularly well-suited for monolithic integration and do not require magnetic components. SC converters can operate under zero load conditions without needing artificial loads or complex control mechanisms. When fully discharged, the output voltage of an SC converter is determined solely by its architecture. Furthermore, power losses can be minimized to zero by reducing the switching (clock) frequency, while still maintaining excellent no-load output voltage control.

Applications such as electric vehicles, battery equalization circuits, voltage-balancing circuits for multilayer inverters, and power supplies for mobile electronic systems can greatly benefit from the Switched Capacitance principle. Compared to traditional switched-mode power supplies, SC power converters can achieve a substantial reduction in size. They are made up of switches and capacitors, eliminating the need for magnetic devices. In addition, the behaviour of these circuits can be characterized by simple equivalent circuits. These converters can be produced on an integrated circuit (IC) chip for semiconductors.

One issue that arises with SC converters is the need to ensure consistent control of the output voltage, even when faced with substantial changes in load and fluctuations in the input voltage[23]. Endless voltage regulation can be achieved, but it comes with a trade-off of reduced converter efficiency. The power stage losses of SC converters rise as the load increases, and SC converters exhibit a non-zero output resistance even with ideal components. Practical limitations on capacitor and switch size restrict SC converter applications to lower and medium power levels, typically in the range of several tens of watts. SC converters are commonly utilized alongside switch-mode inductive-capacitive converters.

Fig. 2.7 displays a popular SC converter that amplifies the input voltage. This converter is equipped with 13 switches and 5 capacitors. The switches are operated by a two-phase, non-overlapping clock, where each switch is turned on during either Phase 1 or Phase 2. In practical applications, diodes can sometimes be used as replacements for certain switches. When switch 1 is turned on, all capacitors, except for the output capacitor, are connected in parallel to the input voltage source V. When switch 2 is turned on, the

capacitors connected in series with the V supply will charge to the output. Upon inspection, it is found that the initial voltage (Vo = 5Vg) and the voltage across the capacitors remain constant in a direct current (DC) state when the converter is not under any load.

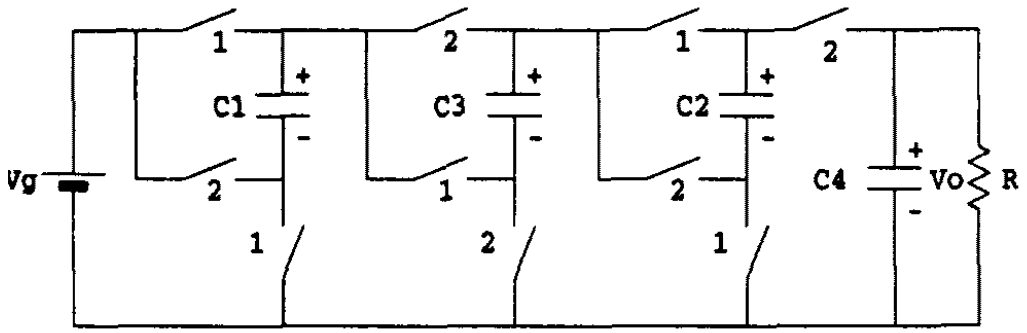

Figure 2.8 : A step-up conversion using a SC converter with four capacitors, achieving the ideal conversion. ratio *M* = *Vo/Vg* = 5.

2.4 Ratio of voltage conversion

For the calculation of the ideal dc conversion ratio, Mi = Vo/Vg, in the absence of any load on the converter. Figure 2.8 provides an illustrative example to clarify the subject matter. Figure 2.9 shows the two switched networks of this converter, which correspond to the two clock phases.

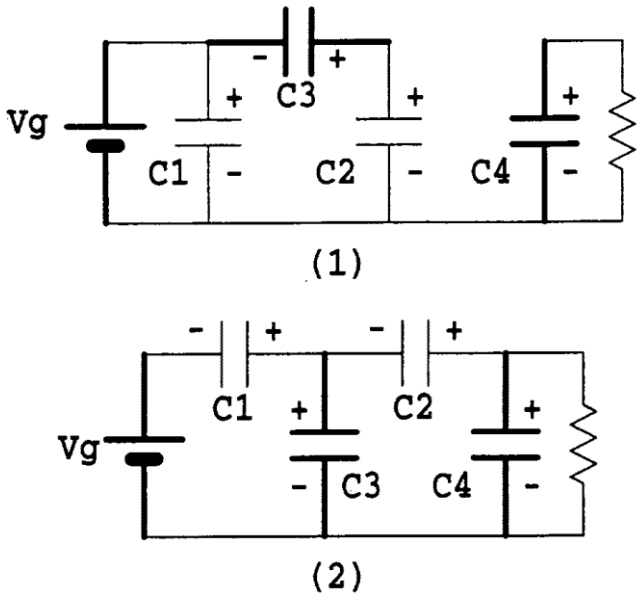

Figure 2.9 : Represents phases 1 and 2 of the clock. Highlighted are the twig branches.

For an Switched Capacitance converter working at no load, the ratio is:

$$Mi = V_o/V_g = P/Q \tag{2.21}$$

where P and Q are values that are solely determined by the configuration of the capacitors in the SC networks. When all the dependencies on various factors like capacitances, switch resistances, switching frequency, clock duty ratios, etc. are eliminated and finding conversion ratio becomes purely topological in nature.

From fundamental loop matrices we get the capacitor interconnections in the two switched networks allowing us to derive a general expression for the optimal conversion ratio. There are a total of k + 1 capacitors and voltage source Vg. Every SC network (j = 1, 2) has $k_t(j)$ capacitor twigs that join the source V, twig to create a tree, and linkages are represented by h (j) = k - kt(j) for capacitor branches. For each of the two networks, k~(j) independent voltage-loop equations can be written. We require a total of k independent equations in order to obtain a unique solution for k capacitor voltages, thus the two switched networks must meet the following requirements:

$$k_i(1) + k_i(2) = k_t(1) + k_t(2) = k \tag{2.22}$$

In each of the two networks shown in Fig 2.8, the highlighted branches represent the switched networks. There are 2 capacitor links (kl) and 2 capacitor twigs (kt) in each network. Observing system of two fundamental-loop matrices: Bf(l) for the network in phase 1 and Bf(2) for the network in phase 2. The matrix Bf(j) has dimensions of kl(j) and x (k + 1). If we arrange the elements in the following order: kl(j) capacitor links first, kt(j) capacitor twigs second, and the V, twig last, the fundamental loop matrix for both network is as follows.

$$B_f(j) = [U(j)B_t(j)b(j)] \tag{2.23}$$

where Bt(j) is a kt(j) x kt(j) matrix of twig-capacitor connection coefficients, U(j) is a kt(j) x kt(j) identity matrix, and the coefficients in the b(j) vector represent the connections of V. At last, the KVL equations becomes into[23].

$$B\begin{bmatrix} V_C \\ V_g \end{bmatrix} = 0 \tag{2.24}$$

where the system matrix is represented by B = [Bf(1) Bf(2)]^T, and The capacitor voltage vector is denoted by V_C. Regarding a specific SC network, We can solve system (2.23) for every capacitor voltages in within V, similar to [2]. Rather, we utilize the effective approach. method resolving equation (2.23) using the loop's incremental representation formulas that incorporate the two-graph formulation into successive single-graph expression [11]. In this version, link voltages are removed from equation (2.23), resulting in a smaller system is solvable for voltages in twigs. Consider the scenario when k is even as an example, and the Since there are the same amount of twigs in both SC networks the arrangement (2.23) turns into

$$\begin{bmatrix} U & B_t(1) & b(1) \\ U & B_t(2) & b(2) \end{bmatrix}\begin{bmatrix} V_{C1} \\ V_{Ct} \\ V_g \end{bmatrix} = 0 \tag{2.25}$$

where the vectors representing the capacitor link and capacitor twig voltages are, respectively, v_{Cl} and v_{Ct}. When the system is in the incremental onegraph form, it becomes,

$$\begin{bmatrix} \Delta B_t & \Delta b \end{bmatrix}\begin{bmatrix} V_{ct} \\ V_g \end{bmatrix} = 0 \tag{2.26}$$

Keeping in mind that the system ignores every capacitor transient voltages (v_{ct}) in terms of Vg and is of order k/2 (k/2 + 1).

$$v_{ct} = -(\Delta B_t)^{-1}\Delta b V_g \tag{2.29}$$

In the example of figure 2.8 , and figure 2.9, we have,

$$v_{ct} = \begin{bmatrix} V_{c3} \\ V_{c4} \end{bmatrix} = -\begin{bmatrix} 1 & 0 \\ -2 & 1 \end{bmatrix}^{-1}\begin{bmatrix} -2 \\ -1 \end{bmatrix}V_g = \begin{bmatrix} 2 \\ 5 \end{bmatrix} \tag{2.30}$$

Vo = vc4, after analysis we find that converter in Fig. 2.7 achieves the optimal conversion ratio of Mi = 5.

2.5 Controller design for Modified-SEPIC

The controller's goal is to make the battery charger function satisfactorily in both forward as well as in reverse power flow mode. Controller designed here is a dual loop control working for correcting both voltage and current.

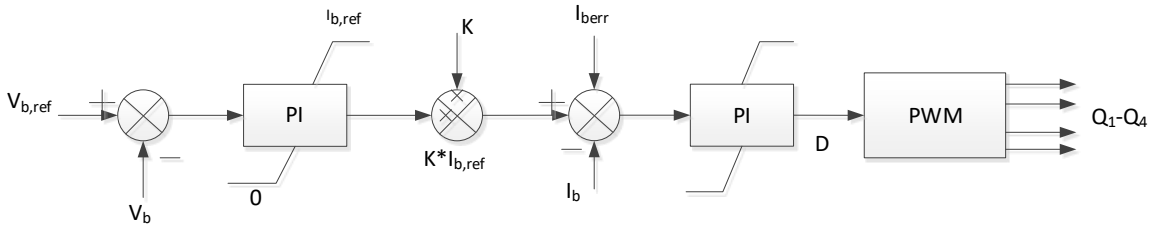

Figure 2.10 block diagram of the controller required

The controller uses a constant to change the operating modes of the converter, having value 'κ'. Forward operation, is indicated by a positive value of "κ," whereas the reverse operation is indicated by a negative value of "κ." As seen in Figure: 2.10, the modified-SEPIC controller monitors and corrects the voltage and current measured of the battery and can also be set to charge or discharge the battery at limited current.

The measured voltage is subtracted from the desired set point which is then given to the PI block , the PI block has its output saturated at rated battery current this output is then subtracted to rated current required which then again passed to a PI block to generate PWM signals which is sampled at the required sampling time to give the switching pulse to the converter.

2.6 Simulation analysis

Through simulation, the suggested battery charger is working at peak voltage of 380V. Additionally, the battery capacity used is 48V 100Ah, Figure 2.10 show simulations under the set parameters.

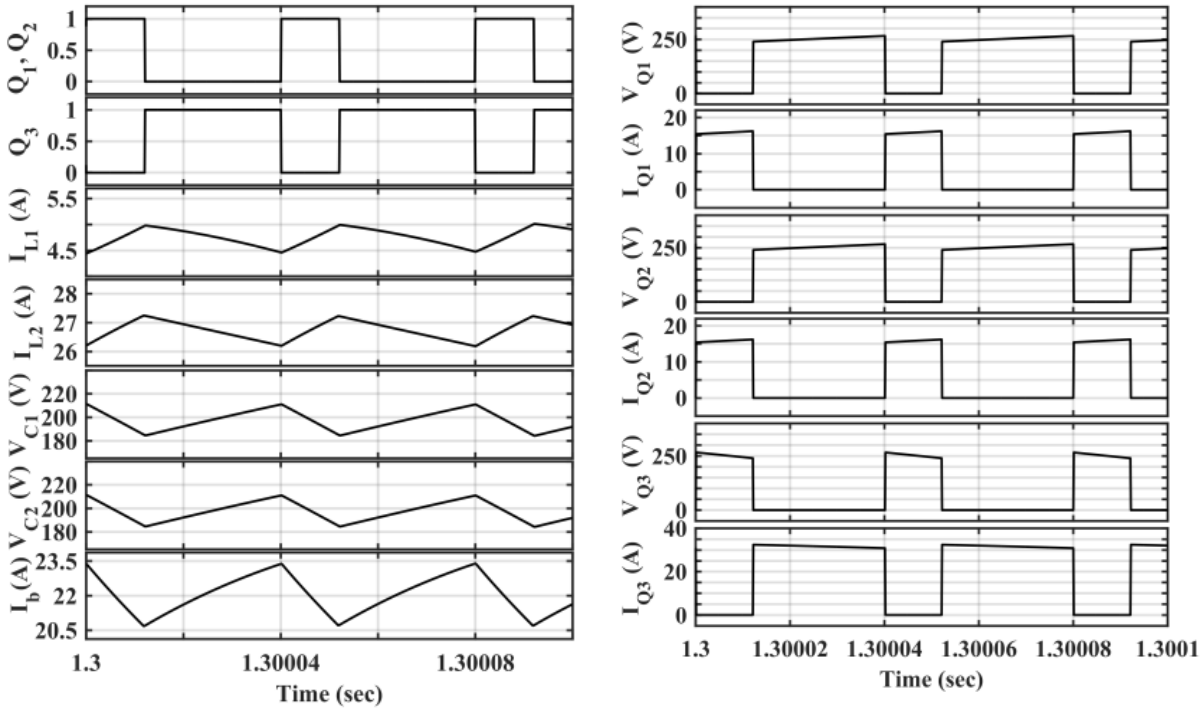

Figure 2.11 Forward mode inductors, capacitors, and switches output waveforms

The output waveform of the inductors and capacitors in Figure 2.11 ensures that the ripples of both the input inductor current and output capacitor are within the desired limit. Therefore, the design of inductors and capacitors for the modified-SEPIC is within acceptable conditions. Figure 2.12 also displays the waveforms for current and voltage of the switch.

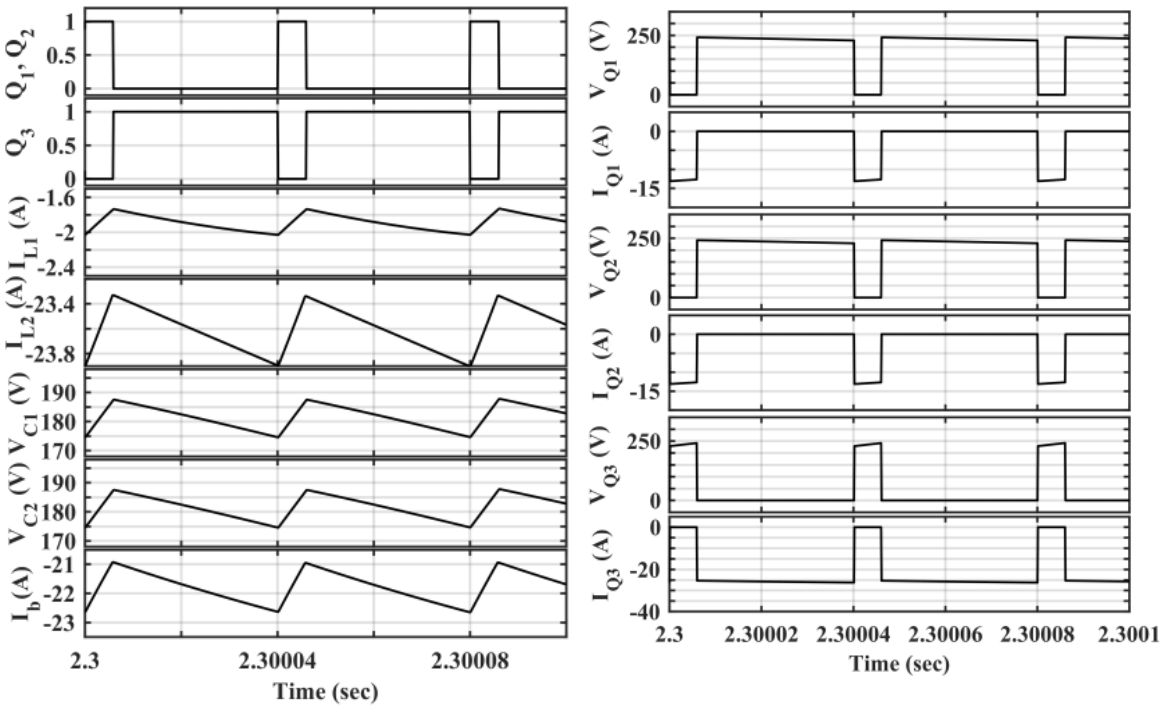

Figure2.12 Reverse mode Switches , capacitors and inductor output waveform

Notably, simulation is used to validate performances during the reverse power flow operation at rated values. The results of this simulation analysis are displayed in Figure. 2.12 as shown in the voltage ripples and current ripples are controlled and the control mechanism is working in proper manner.

As a result, controller design and control are justified hence it is working under rated conditions and the designed bidirectional charger operates satisfactorily during the bidirectional operation.

2.7 Conclusion

This chapter provides the fundamental concepts and mathematical models of Modified-SEPIC. The circuit description, then discussing about the two modes of operation the forward and reverse powerflow mode. The introduction of Switched Capacitance and how to implement it, calculation of Voltage conversion ratio and how can we reduce the switching stresses in our proposed converter in comparison to the traditional SEPIC converter. Designing the controller scheme for converter in which is a dual loop control and utilizes a smart mechanism for power transfer in both direction to work in both CC and CV charging mode adding a constant ‘k’ in the control mechanism to control the flow of power by changing the sign of the constant, then simulation analysis of the modified SEPIC.

CHAPTER 3
DUAL ACTIVE BRIDGE CONVERTER FOR BIDIRECTIONAL CHARGING

3.1 Introduction

Ever since the Dual Active Bridge (DAB) converter's outstanding performance in the previous ten years has led to its meteoric rise in popularity. Voltage boost and buck functions are made possible by power transfers between the energy storage element and the dc voltage bus, which keep the voltage at the dc buses steady. The use of DABs has skyrocketed due to their extensive use in power electronics and industrial applications. These include micro grids, electric vehicles, aerospace energy storage systems, uninterruptible power supplies (UPS), and many more power applications that employ intermediate energy storage systems. Connecting two active bridge converters in a UPS system is shown in Figure 3.1.

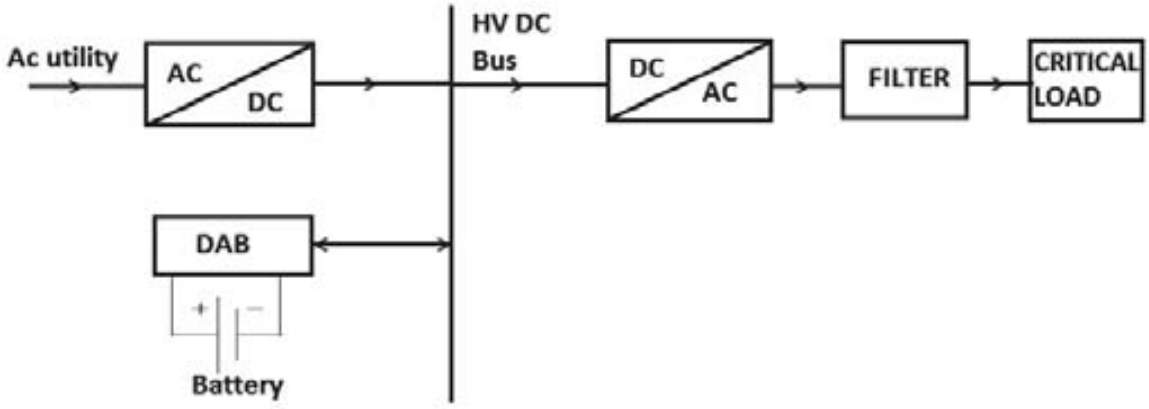

Figure 3.1 : DAB converter block diagram for UPS

In order to modify the direction of power flow, the SPS control method [5] keeps the high frequency transformer's primary and secondary voltages in phase. Researchers have examined many facets of performance and operation for standard control schemes like SPS, as well as for steady state operation, closed loop control, inductor selection, and zero voltage switching (ZVS). According to [8], the DPS control method provides two tiers of

control: first, an external phase shift between the high frequency transformer's main and secondary voltages; and second, an equal internal phase shift between the bridges' cross-connected switches. The use of high-frequency link power conversion systems in DAB control algorithms has been the subject of much research [10]. The effects of step load change, inductor peak current, switch stress, and closed loop operation on circuit design and comparison are investigated in this thesis. Waveforms from the two control strategies—single phase shift and dual phase shift—are compared. The aforementioned control mechanisms can be tested and results obtained through simulation studies conducted in MATLAB and SIMULINK. A single phase Dual Active Bridge topology is shown in Figure 3.2.

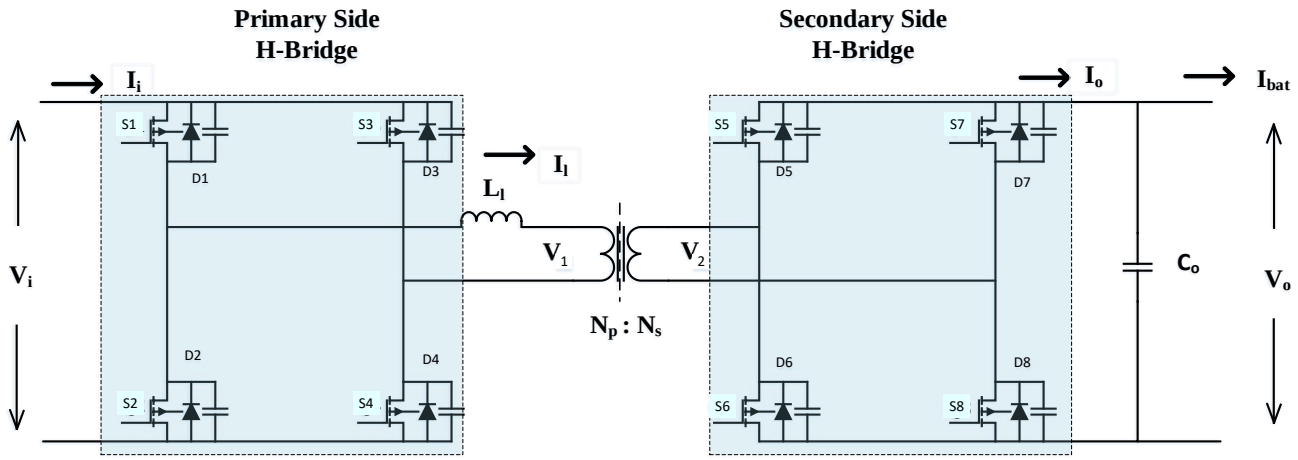

Figure 3.2 : Single phase Dual Active bridge converter circuit description

3.2 Description and system modelling.

The Figure 3.2 shows the converter circuit configuration for the single-phase dual-active-bridge model. S1 and S2 on one leg represent the switches in the primary side H Bridge, and D1 and D2 on the other leg represent the anti-parallel diodes. S3 and S4 are the switches in the second leg [5]. The matching anti-parallel diodes are D3 and D4.On the other side, S5 and S6 are the secondary side H bridge switches, and D5 and D6 are the anti-parallel diodes that correspond to them. The switches in the second leg are S7 and S8, and the associated anti-parallel diodes are D7 and D8. Two bridge converters linked by a high frequency transformer make up the system, as depicted in the image. The primary side leakage inductance is represented by the inductor (L), whereas the secondary side inductor is the same thing. Control pulses with a duty ratio of 50% are used to operate the switches. The terminals across the HF transformer produce voltages that are square waves with high frequencies. Power flows in the opposite direction of the phase shift in a transformer, from the higher-phase voltage side to the lower-phase voltage side.

3.3 Single Phase Shift Modulation (SPS)

As shown in Figure 3.2, the relationship between the primary voltage, V1, and secondary voltage, V2, of the DAB power converter's transformer—which transfers power from the high voltage side to the low voltage side—is as follows [12]:

$$P = \frac{V_1 V_2}{n\omega_s L_{eq}} \theta\left(1 - \frac{\theta}{\pi}\right) \tag{3.0}$$

This equation can be paraphrased as follows: the power converter inductor, ws, is the phase angle difference between voltages V1 and V2, and 1:n is the transformer's transformation ratio. The DC connection of the grid-tied inverter (400V, for example) and the DC link of the hybrid system (photovoltaic terminals, for example) might be represented by the high voltage port, V1. The low voltage port V2 can be utilized for energy storage using a battery or ultra-capacitor (48V).

3.3.1 BUCK operation Forward mode

Under buck operation, current flows from high-voltage port V1 to low-voltage port V2. By angling the HV side's produced gate pulses toward the LV side, power flows from the main to the secondary in this mode. Both bridges' switching durations and the voltage and current waveforms of the analogous inductor are shown in Figure 3.3. Table I displays the states of the devices that switch on and off. In this mode the phase shift is positive[22].

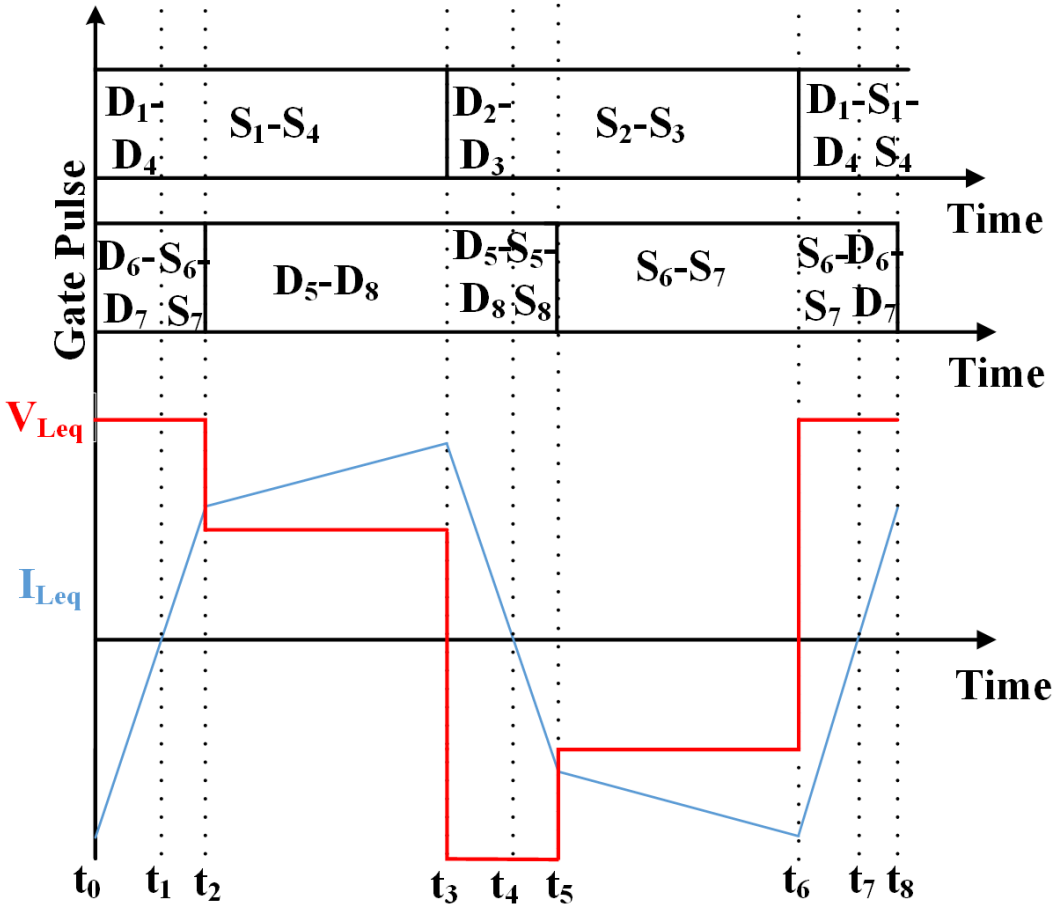

Figure 3.3 : Inductor voltage and inductor current for buck in SPS mode

Table I

Switching States of Converter in BUCk mode

Time Interval	Conducting devices in Primary Bridge	Conductingdevices in Secondary Bridge
t_0-t_1	D1 & D4	D6 & D7
t_1-t_2	D1 & D4	S5 & S8
t_2-t_3	S1 & S4	D5 & D8
t_3-t_4	D2 & D3	D5 & D8
t_4-t_5	D2 & D3	S6 & S7
t_5-t_6	S2 & S3	D6 & D7

3.3.2 BOOST mode operation (reverse power transfer)

This is a boost operation, and it starts discharging the battery by powering the 400 V DC input connection. When gate pulses are created at the HV side VSC and trail the LV side by an angle, power transfers from the secondary to the primary side in this case. Table II lists the statuses of the devices that switch. Referring to the gate pulses of both bridges, Figure 3.4 shows the voltage and current across the analogous inductor. Along with that the phase shift changes from positive to negative.

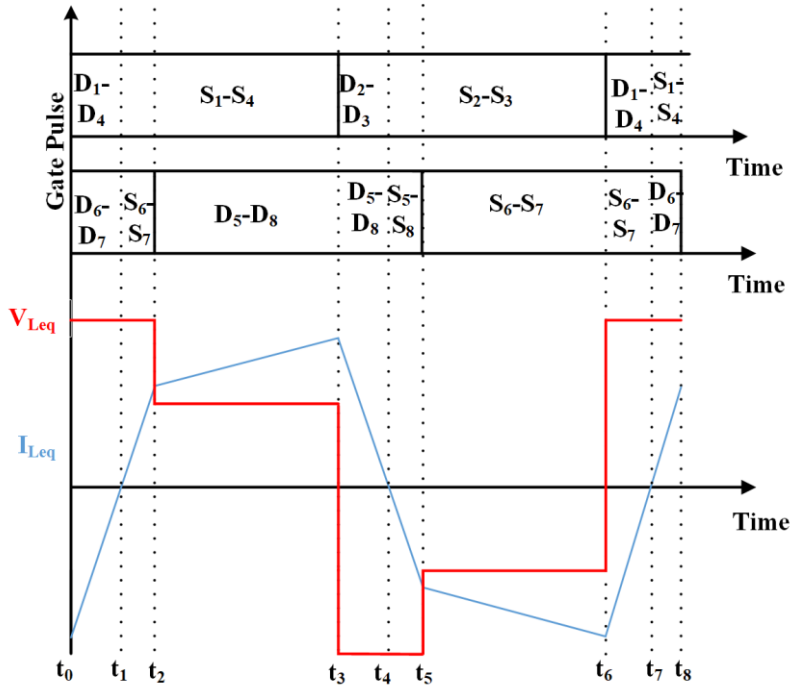

Figure 3.4 Voltage and current waveforms of the inductor in reverse power flow

Table II

Switching States of Converter in boost mode

Time Interval	Conducting devices in Primary Bridge	Conductingdevices in SecondaryBridge
t_0-t_1	S2 & S3	S5 & S8
t_1-t_2	D1 & D4	S5 & S8
t_2-t_3	S1 & S4	D5 & D8
t_3-t_4	S1 & S4	S6 & S7
t_4-t_5	D2 & D3	S6 & S7
t_5-t_6	S2 & S3	D6 & D7

In addition, Figure 3.5 and 3.6 show the waveforms of various electrical parameters such as currents, voltages, and inductor current. These waveforms represent the behaviour of the system during both the charging and discharging modes. During the charging mode, a positive output current means that current is being supplied to the secondary side source[22]. Conversely, a negative input current indicates that current is being drawn from the primary side source. When positive input current is detected, it means that current is being added to the primary side source during the discharge mode. On the other hand, negative output current indicates that current is being taken away from the secondary side source.

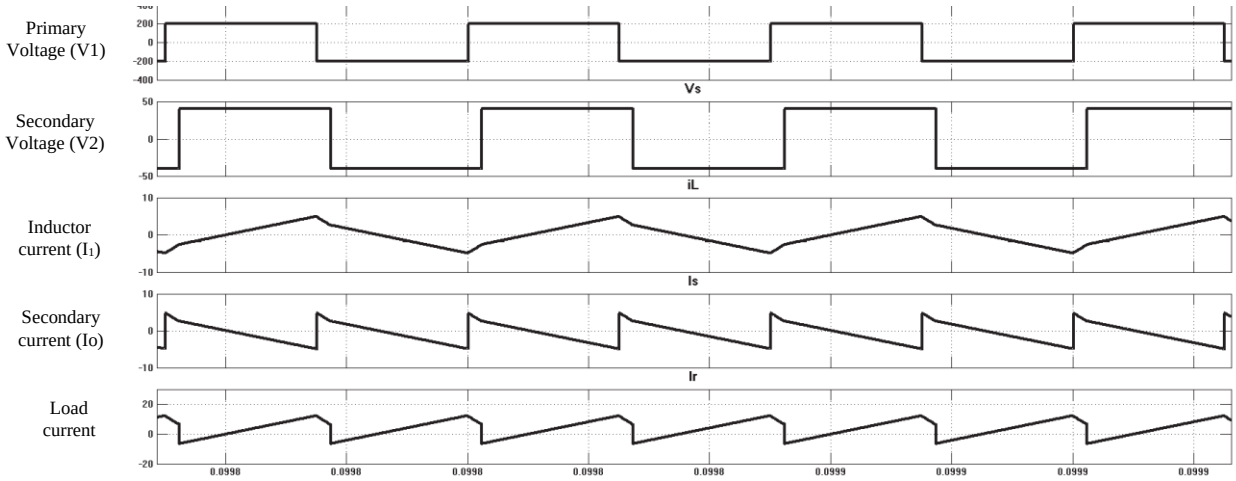

Figure 3.5: primary, secondary and inductor voltages and currents along with Sending and receiving current for forward mode

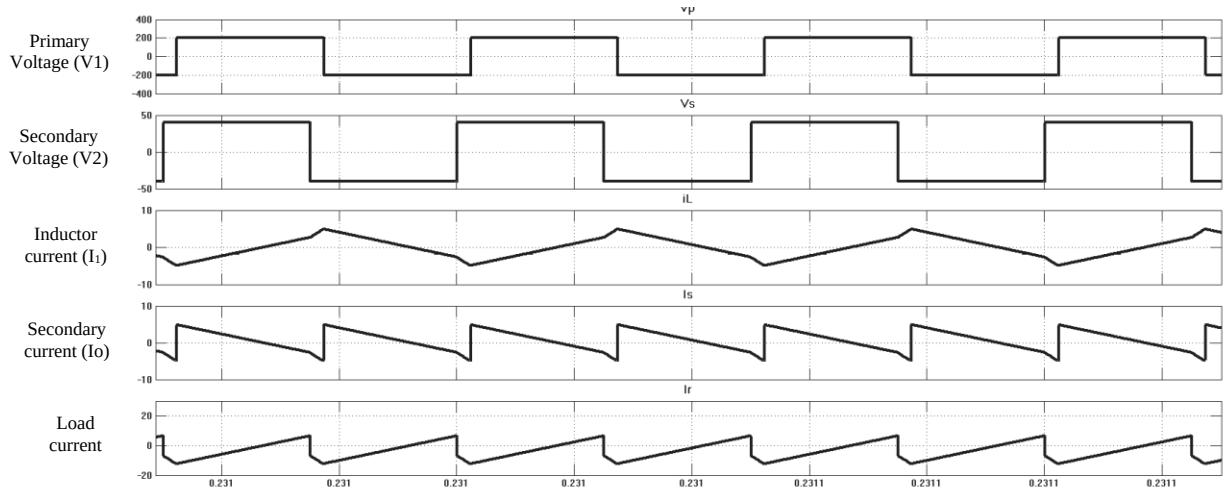

Figure 3.6: primary, secondary and inductor voltages and currents along with Sending and receiving current foe forward mode

3.4 Steady State and Transient Analysis

The DAB converter's steady state analysis is analysed in this topic with proper waveform determining the relationship for the high voltage port current. Fig. 3.7 illustrates this point when the converter is working in forward mode the input varies as $0 < t \le \frac{T_s \theta}{2\pi}$ while the power flow is in forward mode:

$$\Delta I_{in} = \frac{T_s \theta}{2\pi L}(V_1 + \frac{V_2}{n}) \qquad (3.1)$$

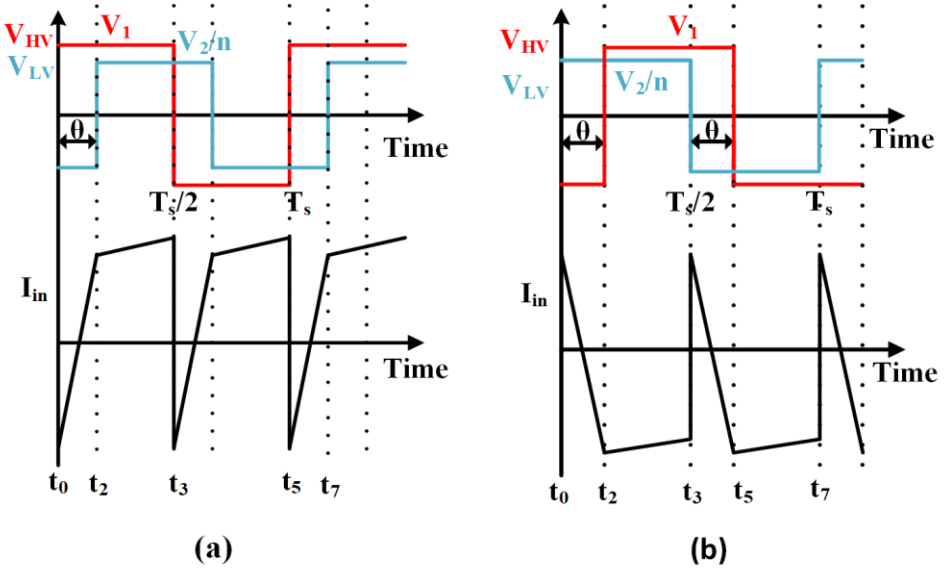

Figure 3.7: (a) Input voltage and current waveforms in buck operation;

(b) Input voltage and current waveforms in boost operation

Where

$$t_2 = \frac{T_s \theta}{2\pi} \tag{3.2}$$

At time instant t2 the input current in the forward mode operation is:

$$i(t_2) = i(t_0) + \frac{T_s \theta}{2\pi L}(V_1 + \frac{V_2}{n}) \tag{3.3}$$

Likewise, the inductor current excursion during the time interval $\frac{T_s \theta}{2\pi} < t \leq \frac{T_s}{2}$ and, consequently, the input port current at t3 can be ascertained as depicted below [23]:

$$I(t_3) = I(t_2) + \frac{T_s \theta}{2\pi L}\left(V_1 + \frac{V_2}{n}\right) \tag{3.4}$$

Where,

$$t_3 = \frac{T_s}{2} \tag{3.5}$$

3.5 DAB Converter's analysis in steady state

With the inductor taken into consideration as an ideal passive element, the input current at time t0 is as depicted following the equation steady state condition i(t3) = i(t0):

$$i(t_0) = \frac{V_2}{n}(1 - \frac{2\theta}{\pi})\frac{T_s}{4L} \tag{3.6}$$

Using equation 3.3 and 3.6, the input port current at port t2 is:

$$i(t_2) = [\frac{V_2}{n} - V_1(1 - \frac{2\theta}{\pi})]\frac{T_s}{4L} \tag{3.7}$$

Moreover, the following can be established about the input port current's behaviour:

$$i_{La}(t) = i(t_0) + \frac{i(t_1) - i(t_0)}{\frac{T_s \theta}{2\pi}} t \quad ; \; t_0 < t < t_2 \tag{3.8}$$

$$i_{Lb}(t) = i(t_1) + \frac{i(t_2) - i(t_1)}{\frac{T_s}{2\pi}(1 - \frac{\theta}{\pi})} t \;;\; t_2 < t < t_3 \tag{3.9}$$

As a result, the input source (port) current average is:

$$i_{inavg} = \int_0^{\frac{T_s\theta}{2\pi}} i_{La}(t)dt + \int_{\frac{T_s\theta}{2\pi}}^{\frac{T_s}{2}} i_{Lb}(t)dt \tag{3.10}$$

$$i_{inavg} = \frac{V_2}{2n\pi f_s L}\theta(1 - \frac{\theta}{\pi}) \tag{3.11}$$

3.6 Simplified Transient model

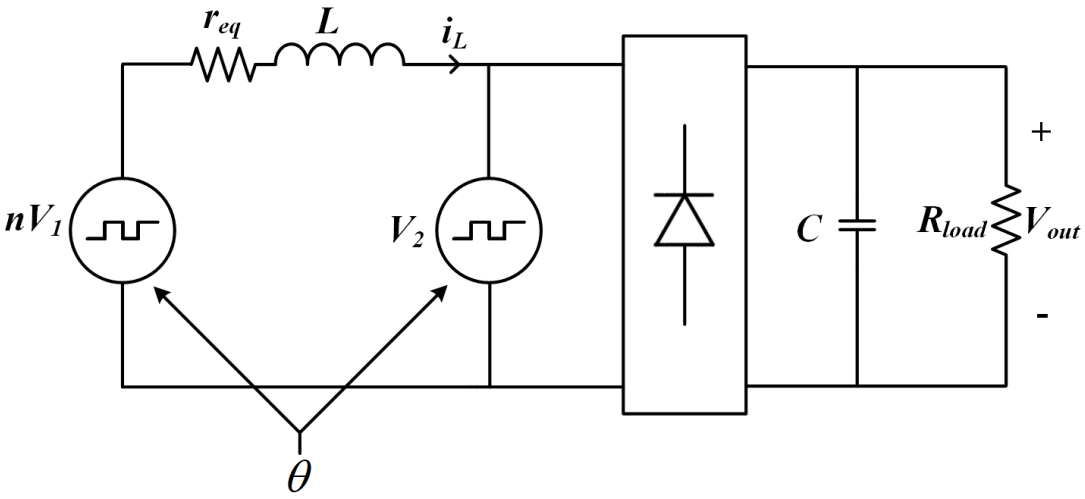

Figure 3.8: Equivalent circuit Model of DAB Converter

By establishing a relationship between the input high voltage side port current and the inductor current, this subsection suggests a simplified model of the DAB converter. Figures 3.7(a) and (b) demonstrate that all of the information on the effect of phase shift on inductor current is present in the input high voltage side port current throughout half of the switching cycle[22]. This finding showed that phase shift analysis of the inductor current regulation

may be done utilizing the port information.

Figure: 3.8's comparable circuit is utilized in the model-building process. The output port is changed to the corresponding load R-load, as seen in the figure. The resistance of the effective inductance L (including transformer leakage) and the converter loss with respect to the secondary side is known as the equivalent resistance, or r_{eq} .In the event of forward transfer of power, the state space model within the interval $0 \le t < \frac{T_s \theta}{2\pi}$ is

$$\begin{bmatrix} \dot{i}_L \\ \dot{v}_2 \end{bmatrix} = \begin{bmatrix} \frac{-r_{eq}}{L} & \frac{1}{L} \\ \frac{-1}{C} & \frac{-1}{RC} \end{bmatrix} \begin{bmatrix} i_L \\ v_2 \end{bmatrix} + \begin{bmatrix} \frac{n}{L} \\ 0 \end{bmatrix} v_1 \quad (3.12)$$

As similarly, the model that applies at time $\frac{T_s \theta}{2\pi} \le t < \frac{T_s}{2}$ can be expressed as follows:

$$\begin{bmatrix} \dot{i}_L \\ \dot{v}_2 \end{bmatrix} = \begin{bmatrix} \frac{-r_{eq}}{L} & \frac{-1}{L} \\ \frac{1}{C} & \frac{-1}{RC} \end{bmatrix} \begin{bmatrix} i_L \\ v_2 \end{bmatrix} + \begin{bmatrix} \frac{n}{L} \\ 0 \end{bmatrix} v_1 \quad (3.13)$$

A simple model for a DAB converter is built as follows, with the analogous circuit depicted in Fig.3.8, using the averaging technique for finding state space equation for half the switching cycle and finding the phase shift relation as $d = \frac{\theta}{\pi}$

$$i_L = \frac{-r_{eq}}{L} i_L - \frac{(1-2d)}{L} v_2 + \frac{n v_1}{L} \quad (3.14)$$

$$\dot{v}_2 = \frac{(1-2d)}{C} i_L + \frac{1}{RC} v_2 \quad (3.15$$

3.7 Control Strategy of DAB Converter

By rearranging (3.14), the equations produces the transfer function of the plant as follows

$$\frac{I_L(s)}{m(s)} = \frac{1}{sL + r_{eq}} \tag{3.16}$$

Hence the control variable is defined as d, is related by m where 'm' is the error of the PI block and 'n' is the turns ratio of transformer.

$$m = -(1-2d)V_2 + nV_1 \tag{3.17}$$

Capacitors are used to sustain both ports in order to either lessen source stresses or ripple current at load.
Because the port voltage variations in the inner current loop are sufficiently slow in relation to the current control bandwidth, feed-forward compensation can be applied to their average values as follows:

$$d = \frac{m - nV_1}{2V_2} + \frac{1}{2} \tag{3.18}$$

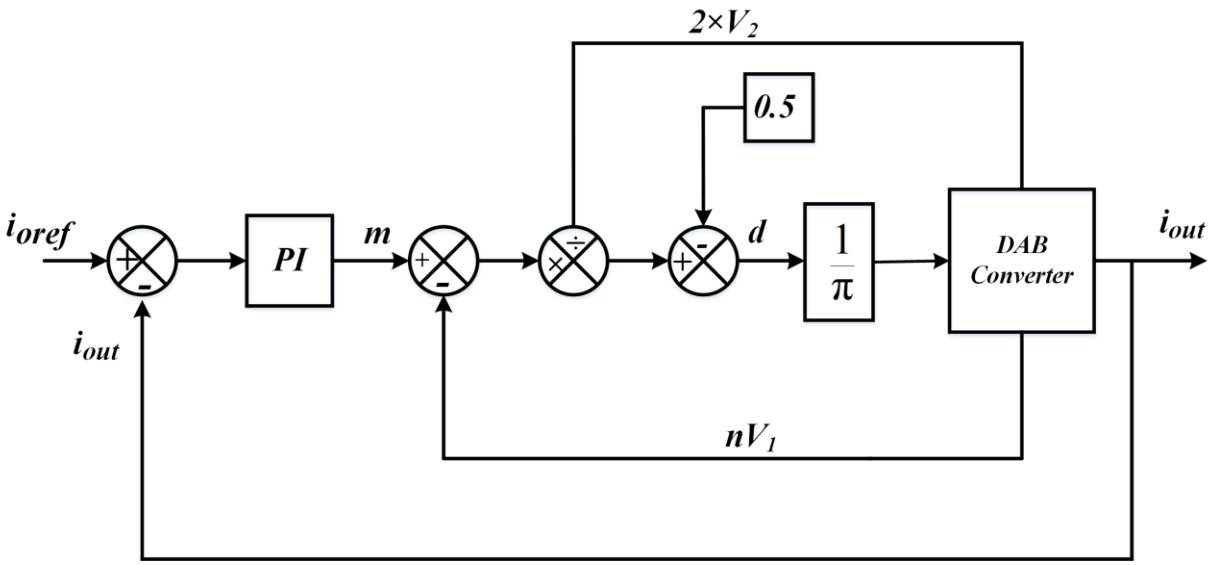

Figure 3.9: The current control loop of DAB Converter

A DAB bidirectional converter's objective is to regulate the power distribution between the low voltage and high voltage ports, and one way to do this is by the use of port current control. As mentioned in the preceding subsection, the relationship between equivalent inductor current and port current has been shown. A proportionate-integral (PI) compensator is used to process the error signal between the reference set point and the current at the output port in order to construct the control variable m. Then, using the feedforward compensation that is established in (3.17), this control variable can be transferred. In order for the PI zero, denoted as s = πKi=Kp, to offset the improperly positioned plant pole, the PI compensator, Gc = Kp + Ki, can be configured for the plant transfer function (3.16).

To set the bandwidth limit at $f_{Ci} = \frac{1}{10} f_s$, the loop transfer function's time constant is changed. The following two situations result in the PI values:

$$K_i = \frac{r_L}{\tau} \;\; ; \;\; K_p = \frac{L}{\tau} \tag{3.19}$$

Where , $\tau = \frac{1}{2\pi f C_1}$

In DAB, the phase shift between the bridges is calculated using the delay d and variable m, which guarantees a zero steady state error. Figure.3.7 depicts the whole control approach

3.8 Simulation Result

By simulating the DAB converter in MATLAB-Simulink, we can confirm that the proposed simpler model for this converter works as intended and that the feedback loop control that is based on this topology performs dynamically well. The simulation uses the high-frequency transformer as its model, assuming it has no core losses and using its equivalent impedance as series inductance. The parameters of the system are presented in below. The associated simulation results for the closed-loop bidirectional DAB converter are discussed in this section.

Table III

Parameters used for calculation

Simulation parameter	Value
Input Voltage (Vin)	400V
Output Voltage (Vb)	48V
Switching frequency (fs)	20kHz
Equivalent resistance (Req)	10 m Ω
Equivalent Inductance (Leq)	46.22 μ H
Filter Inductor (Lf)	7.23nH
Filter Capacitor (Cf)	1000 μ H
The input capacitor (C1)	100 μ H
Transformation ratio	3:25
Power rating of Transformer	10KVA

A 400 V source is required to stimulate the bidirectional DC-DC converter's input port. Both bridges have a 50% duty period and operate with a 180° phase angle between each of its legs. The control method of the converter provides the phase shift θ, as a control

parameter [Fig. 7]. The bridge converter causes two levels at ± 400 V to switch between them instantly. The low voltage side has the same impact, which leads to periodic ± 48 V pulse train. The switching frequency, fs, is the same as the frequency of the primary and secondary periodic pulses. Between the bridges' reference legs, the phase shift caused by the control scheme is introduced. The outcomes are displayed in Figure: 3.10.

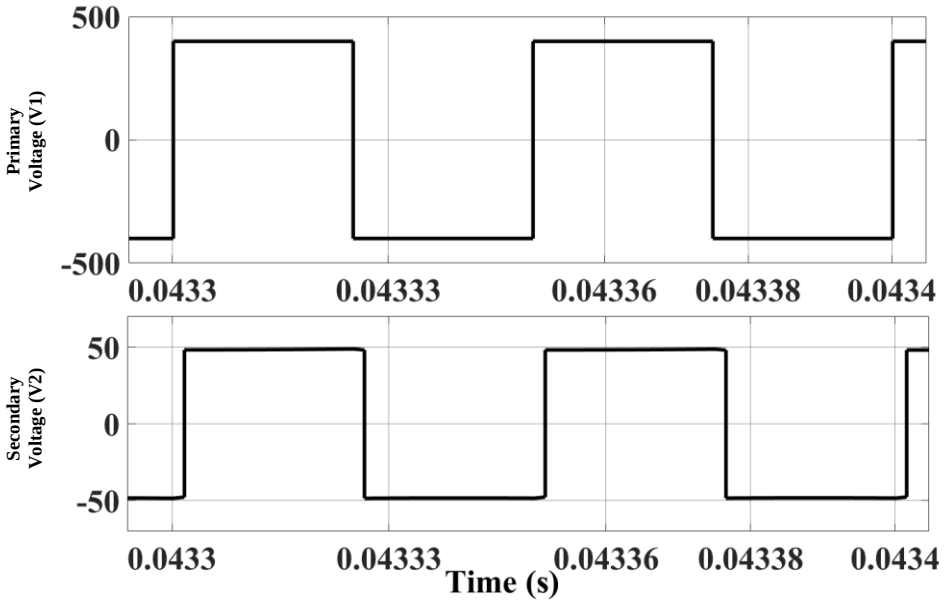

Figure 3.10: Input voltage and output voltage across transformer

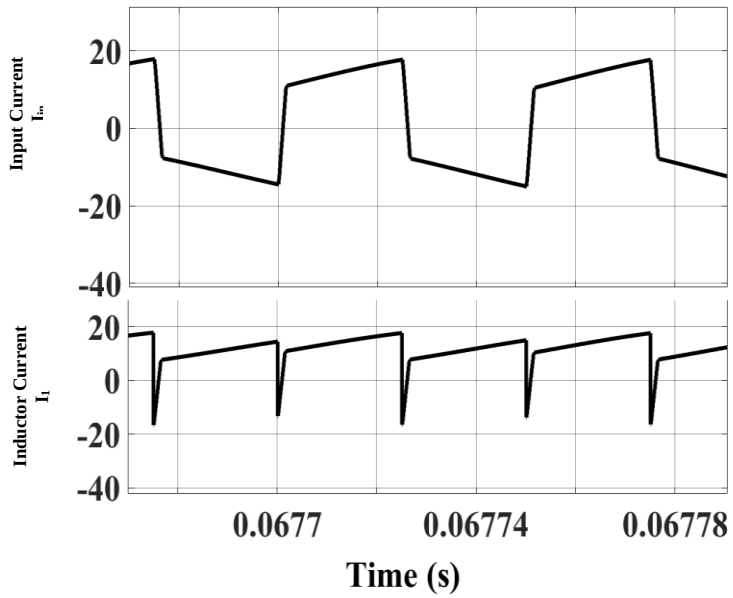

Figure 3.11: Convertor input current while in Buck mode; Convertor inductor current while in Buck mode

As illustrated in Figure. 3.8, under steady state conditions, the main voltage leads the secondary voltage when the control is given a positive current reference, which corresponds to the buck mode. Figure. 3.9 displays the port current and the instantaneous inductor current. As demonstrated in Figure. 3.10, the positive value of the actual current at the low voltage port indicates the power transfer from the high voltage port to the low voltage port. Additionally, it displays the performance reference monitoring in steady state conditions. The real current, devoid of steady state error, tracks the reference value of 100A.

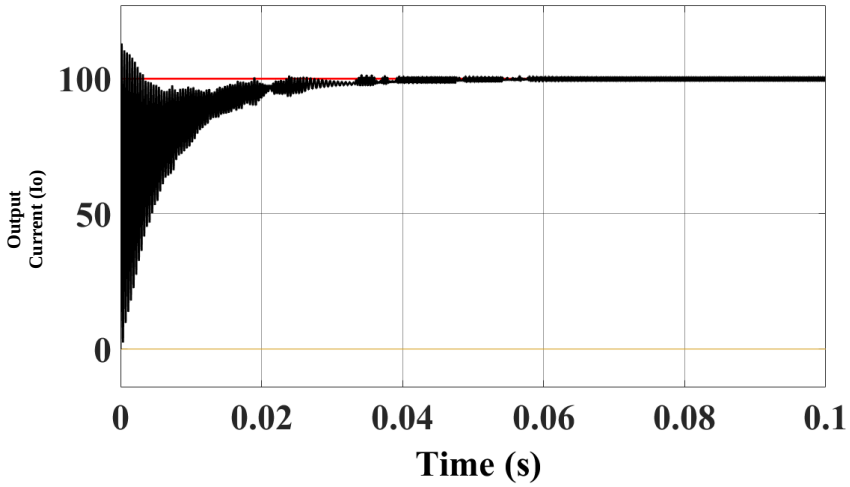

Figure :3.12 Converter output waveform in step down mode

Figure. 3.9 illustrates the noticeable waves in the output current. Regrettably, even at low power transfer, ripple current has a significant value, making port filtering essential. As illustrated in Figure. 3.11, the phase shift of the high voltage side bridge converter lags after that of the low voltage port under negative current reference. Figure 3.12 displays the port current as well as the inductor current. The negative reference current of Ioref = -100 Amp is followed by the real current and reaches zero steady state error, as seen in Figure. 3.13.

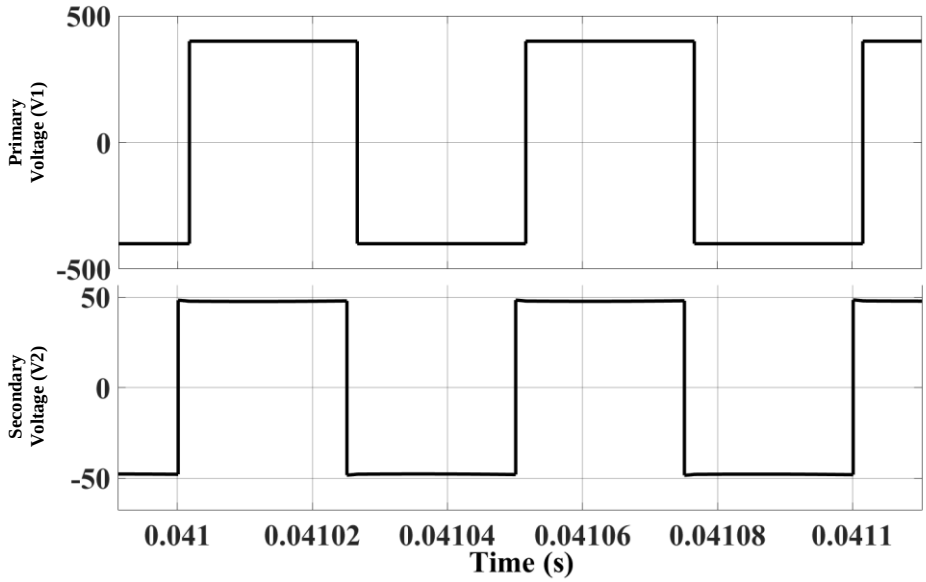

Figure 3.13 Input and output voltage across transformer in boost mode

Lastly, an assessment is made of the close loop control system's dynamic performance. Figure: 3.16 displays the Bode plot of the plant transfer function and the open loop plant transfer function with compensator. It displays the control bandwidth in rad/sec, which is approximately one tenth of the switching frequency.

The controller receives the step input reference in order to change the current from 80 amps to 40 amps at time instant t = 0.05 seconds. As seen in Figure 3.17, the real current follows the reference current within the intended rising time. In Figure: 3.17, the error response is also displayed. The developed control approach and the model that is being presented are validated by the tracking performance.

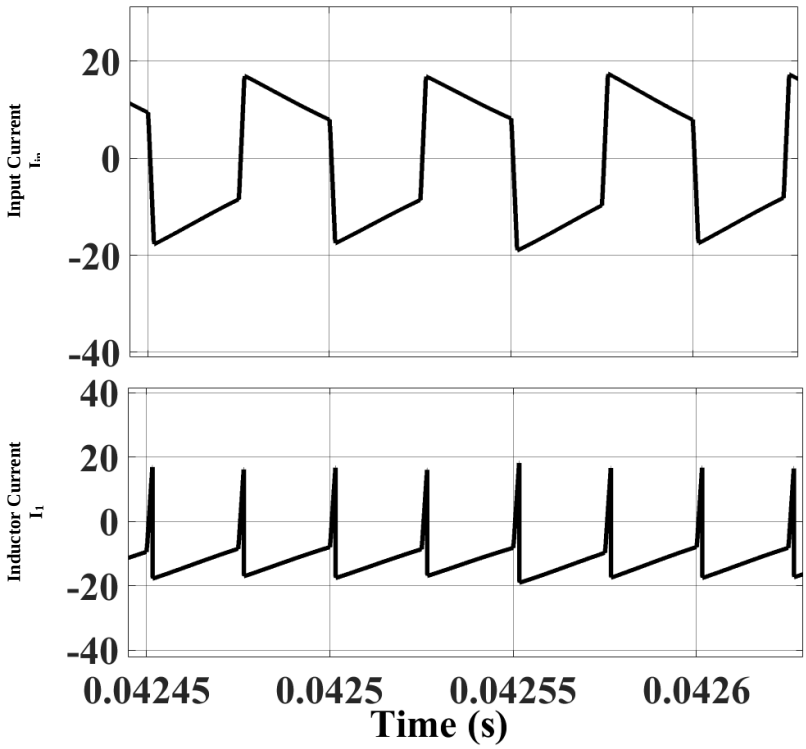

Figure 3.14 Current flowing through the converter's inductor when it is operating in boost mode; (b) Current flowing into the converter when it is operating in boost mode

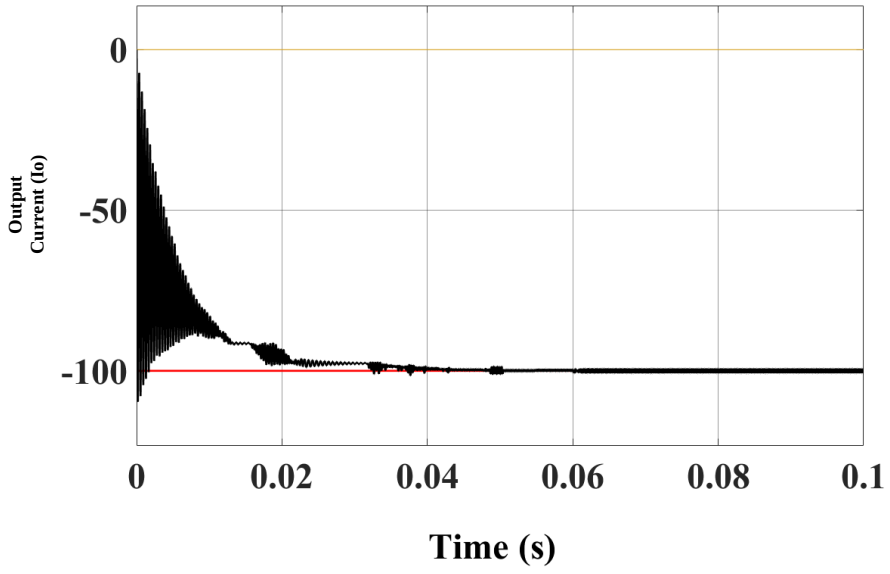

Figure 3.15 Output current of Converter in Boost mode

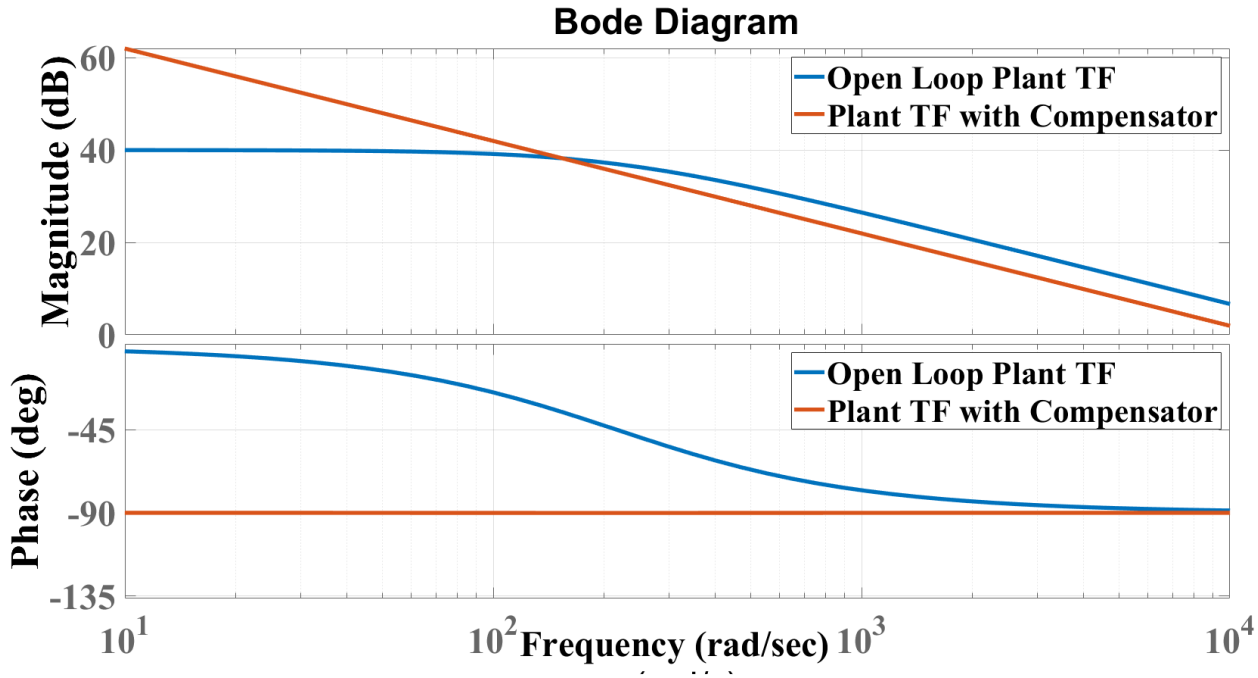

Figure 3.16 Bode Plot

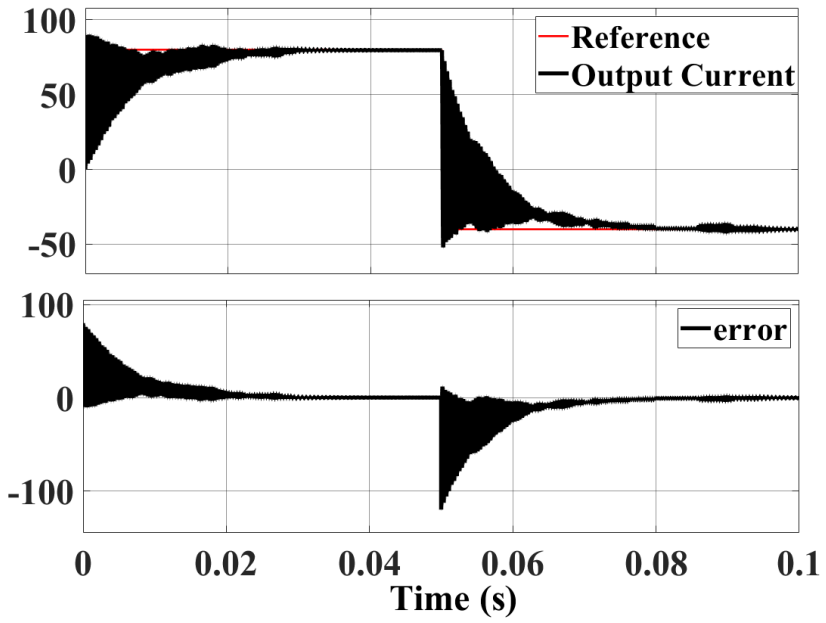

Figure 3.17 Output current with Step reference

3.9 Conclusion

The Dual Active Bridge (DAB) power converter's simplified state-space average model, which removes the complexity of the Fourier-based model, is presented in this chapter. System of excitation by transformer. For the bidirectional converter, a multiple loop voltage control strategy and a current control strategy were developed using the suggested model. The model developed in this study is readily applicable to bi-directional converter topologies utilized in fuel cell applications, solar water pumping projects, charging electrical car batteries, and other applications where voltage ports with significant voltage differences are encountered. Bidirectional converters with galvanic isolation are becoming more and more popular in various power applications because of their lightweight, decent efficiency, and desired fast design turnover.

The formulation of control strategies and compensator designs are based on the simplified DAB converter model. Simulations are used to validate this model and parameters that were obtained analytically. This work includes all pertinent simulation findings to support the validity and effectiveness of the suggested DAB converter model. With the help of its simplified model, the work provided in this study offers guidelines for close-loop control design for a number of additional DAB power converter applications.

CHAPTER 4

DESIGN CALCULATIONS AND MATLAB SIMULINK SIMULATION RESULTS

4.1 Design calculations of Modified SEPIC Converter

To design the passive components of the converter that is being described, the duty ratio of the converter is estimated. Considering the context of a V_B=48 V battery being charged continuously and V_{DC} is the DC bus voltage, the duty ratio is estimated using (2.10).

$$D = \frac{2V_B}{2V_B + V_{DC}} = \frac{2 \times 60}{(2 \times 60) + 380} = 0.24 \tag{4.1}$$

The peak voltage of the battery measured while in constant current (CC) charging mode is denoted by VB in this instance. The duty ratio that was computed is 0.24. The 30% and 15% permitted inductor current ripple, or ΔiL1 and ΔiL2, is what the inductors L1 and L2 are intended to handle. The following equations have been constructed, with values estimated, using (2.1)–(2.9) and the volt–sec balance.

$$L_1 = \frac{DV_{DC}}{2 f_{sw} \Delta i_{L_1}} = \frac{0.24 \times 380}{2 \times 25000 \times 0.3 \times (1100/380)} = 2.1mH \tag{4.2}$$

$$L_2 = \frac{(1-D)V_B}{f_{sw} \Delta i_{L_2}} = \frac{(1-0.24) \times 60}{25000 \times 3} = 0.6mH \tag{4.3}$$

Here, f_{sw} denotes the DC/DC converter's switching frequency. Furthermore, inductors L1 and L2 are calculated to be 2.5 mH and 0.8 mH, taking into 1.25 times factor respectively [24].
The following formulas for C1 and C2 are obtained from (1)–(10), proving that the capacitors C1 and C2 are the same. Therefore, the projected values of capacitors for a voltage ripple content of 25% in these capacitors are as follows.

$$C_1 = C_2 = \frac{2(1-D)P}{V_{DC} f_{sw} \Delta v_{C_1}} = \frac{2(1-0.24) \times 1100}{380 \times 25000 \times 0.25 \times 190} = 3.71\mu F \tag{4.4}$$

Therefore, 4 μF is the chosen value for each of the capacitors, C1, and C2. The design of the passive components must be complemented by the choice of switching devices. The voltage stresses across Q1, Q2, and Q3 switches of the modified-SEPIC converter are computed during charging operation and are provided as follows in this view.

$$V_{Q1} = V_{Q2} = \begin{cases} 0 & \text{During mode-I} \\ v_{C1}(n) + V_b & \text{During mode-II} \end{cases} \tag{4.5}$$

$$V_{Q3} = \begin{cases} v_{C1}(n) + V_b & \text{During mode-I} \\ 0 & \text{During mode-II} \end{cases} \quad (4.6)$$

Here, the instantaneous capacitor voltage is denoted as $v_{C1}(n)$. The average capacitor voltage can be obtained as follows from (2.6).

$$< v_{C1} >= V_{C1} = \frac{V_{DC}}{2} \quad (4.7)$$

As a result, the maximum voltage stress across the switches is approximated with a 30% safety margin when the switch (Q1/Q2/Q3) is turned "OFF."

$$V_{Q1} = V_{Q2} = V_{Q3} = 1.3 \times \left(\frac{V_{DC}}{2} + V_B \right) \quad (4.8)$$

4.1.1 Simulink Results and MATLAB circuit

Below is the matlab circuit model of modified-SEPIC:

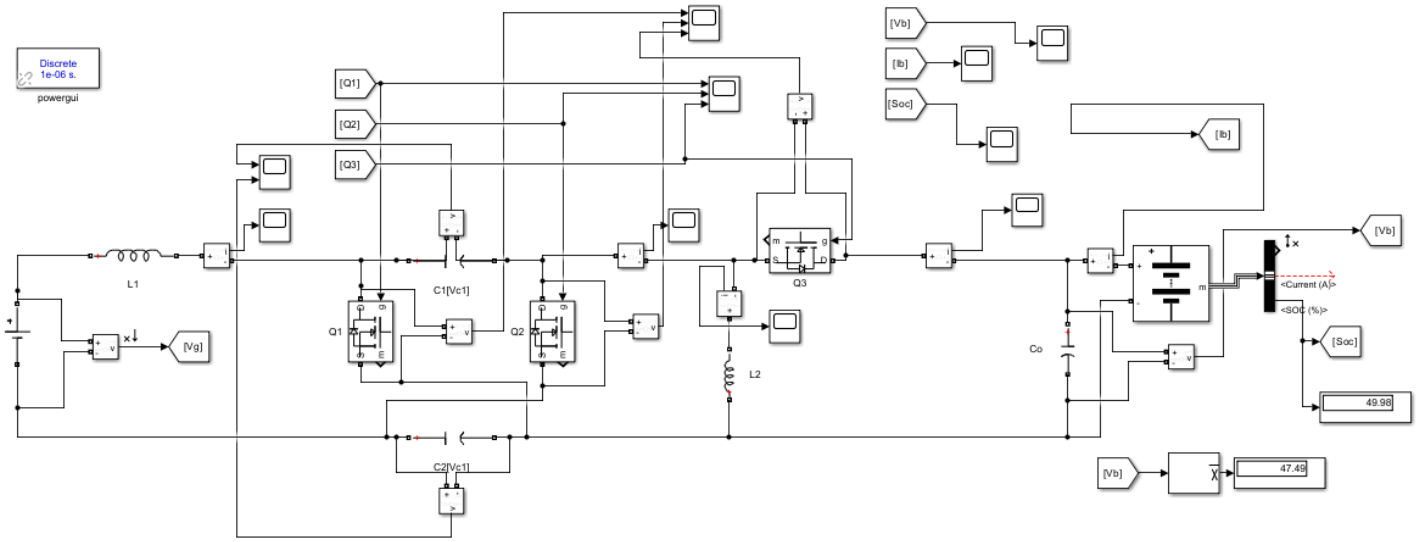

Figure 4.1 : Simulink model of Modified SEPIC

The control strategy used in modified SEPIC is designed si shown below:

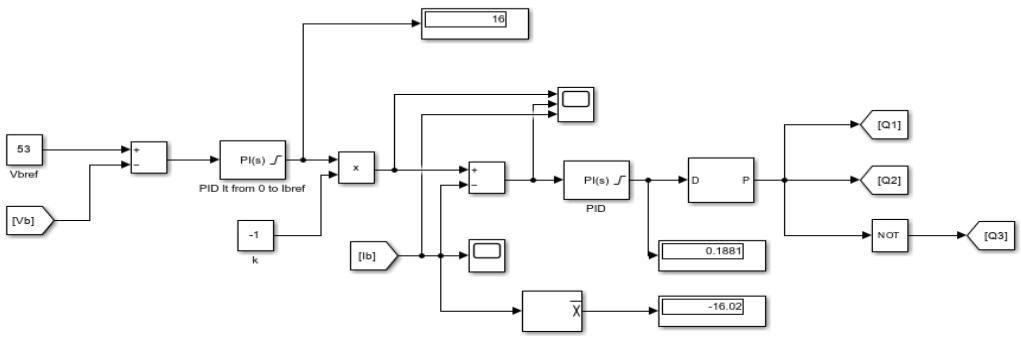

Figure 4.2: Simulink model of control strategy of Modified-SEPIC

Following are the results acquired in matlab Simulink for both Forward mode operation and reverse power flow mode by changing the value of constant ‘k’.

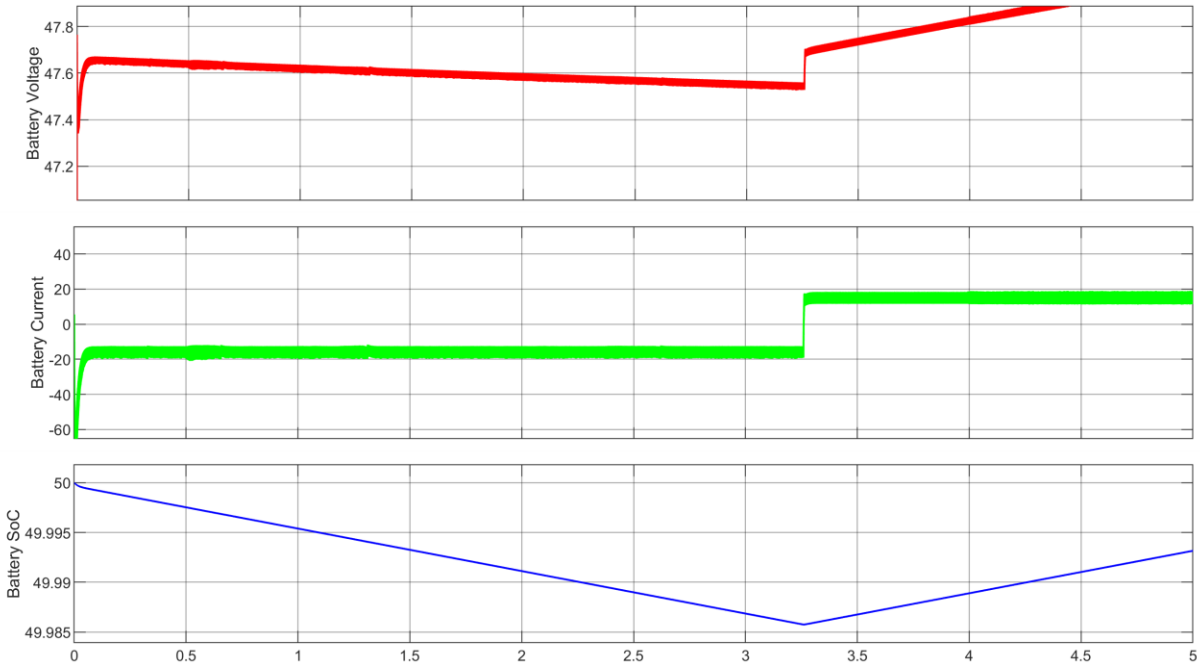

Figure 4.3: Forward and reverse power flow of the Modified SEPIC Converter

The above figure 4.3 shows the forward operation of battery charging in first few seconds from t=0 to t=3.25s , after that changing the value of constant ‘k’ to negative we get reverse power flow showing discharging of battery.

4.2 Design of Dual Active Bridge Converter

As seen in fig. 4.7, the isolated DAB (Dual Active Bridge) converter is made up of two complete bridges coupled by a high-frequency transformer.
One benefit of the DAB is its straightforward operation, which entails using basic square wave signals to operate both bridges simultaneously with a delay between the first and second bridges.

The power that flows through the converter is determined by this delay, which has the following expression [14]:

$$P = \frac{mV_{in}V_o\varphi(\pi - \varphi)}{2\pi L f_s} \tag{4.9}$$

Where, m is the transformer turns ratio
ϕ is the phase delay
f_s is the switching frequency

leakage inductor calculations are as follows:

$$L_l = V_i V_0 \frac{nd(1-d)}{2P_o F_{sw}} \tag{4.10}$$

The waveform of the inductor current is shown in Fig. 5. This waveform can be used to determine the inductor currents il1 and il2.

$$i_{l1} = 0.5(2\phi - (1-m)\pi) I_n \tag{4.11}$$

$$i_{l2} = 0.5(2m\phi + (1-m)\pi) I_n \tag{4.12}$$

Where, m is defined as voltage transfer ratio:

$$m = \frac{V_o}{N V_i} \tag{4.13}$$

The control of the DAB converter requires the transfer function between the phase delay and the output current, which is represented below:

$$G_{id} = \frac{\tilde{i}_o}{\tilde{\varphi}} = \frac{mV_{in}(1-2\frac{\varphi}{\pi})}{2Lf_s} \tag{4.14}$$

4.2.1 Simulink Result and Matlab Circuit:

Figure 4.4 is the matlab circuit of DAB converter, showing two H-bridges with 8 controlled switches 2 for each leg, with having both input and output side Capacitance filter to ensure smooth input and output voltage.

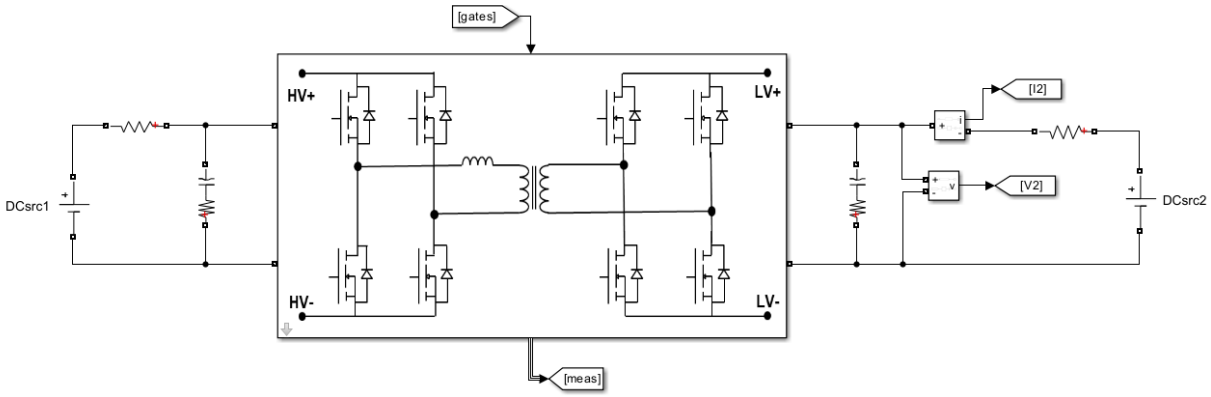

Figure 4.4 Simulink model of Dual Active Bridge

Figure 4.5 shows the control strategy used in the DAB converter , a PI loop is used to find the current error this error is now used to control phase difference between the input side voltage and output side voltage and then pulse generater is used which contains the function to calculates relation between pahse and the gate pulse which then are fed to the switches.

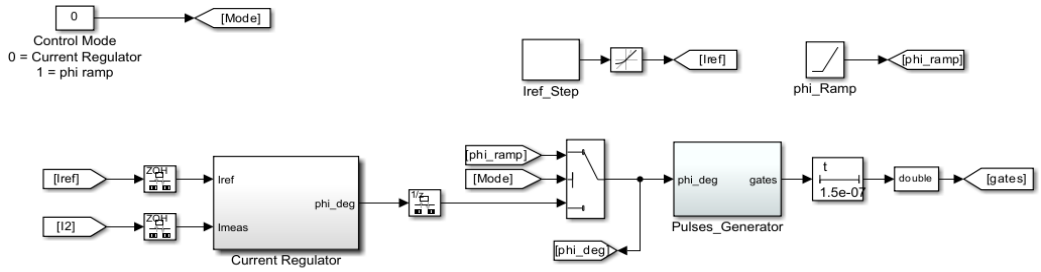

Figure 4.5 Control strategy of Dual Active Bridge

Figure 4.6 shows the respective waveforms of the simulation results, (a) shows the variation of phase and how the variation of phase shows the change in power flow (b) from primary to secondary side of the DAB along with the current flow (c) in both the cases.

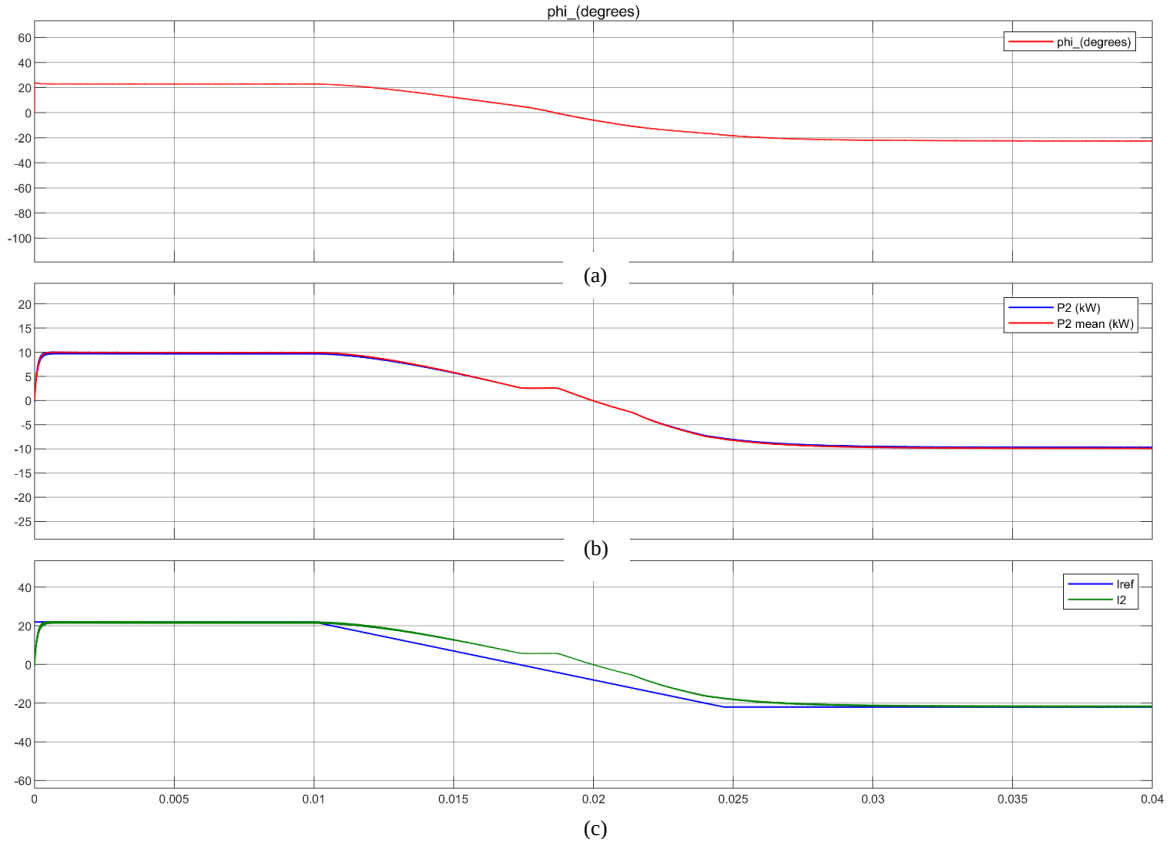

Figure 4.6 (a) Phase variation (b) Power transferred (c) output Current

Figure 4.7 shows the primary and secondary voltages and the inductor current in DAB converter and how the difference in voltages and the phase difference causes the inductor current to follow this pattern.

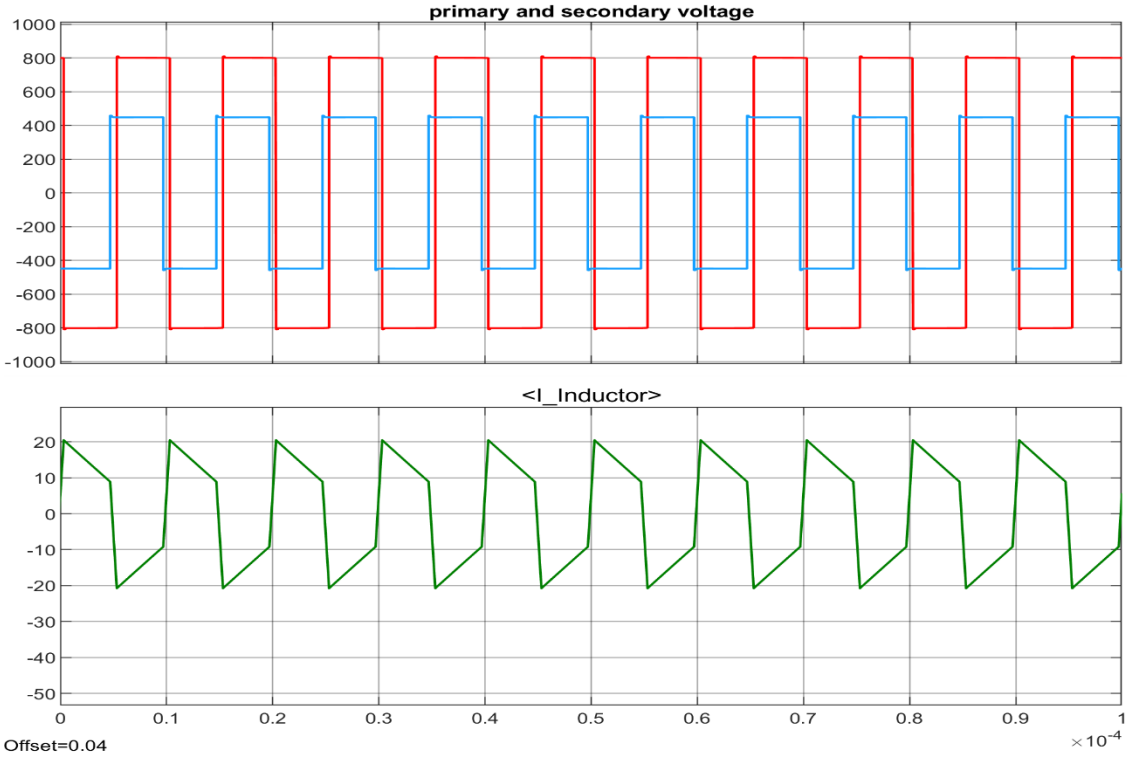

Figure 4.7 Primary voltage secondary voltage and inductor current

4.3 Conclusion

Chapter 4 shows the matlab Simulink results and design calculations, for modified SEPIC how the inclusion of extra switches enables the bidirectional property and decrease the component size, as shown in the design calculations of the presented converter the control block presented here is a dual loop PI controller which adjusts both current and voltage according to the requirements.

This chapter also shows the respective waveform of DAB converter working in both forward power flow mode and reverse power flow mode along with the matlab circuit description the control block is a PI block with phase generator block with proper relation between the phase difference and gate pulse required to give at the switches.

All the output waveforms formed using matlab Simulink and the converter circuit used for simulation is presented in the chapter along with the circuit display of the proposed control block

CHAPTER 5

MAIN CONCLUSION AND FUTURE SCOPE OF WORK

5.1 Main Conclusion

The bidirectional modified-SEPIC charger discussed in this thesis designed for low powered EVs working at 48V and 120V is designed at 1.1kW and can be used for light utility vehicles in the market .How it is different from traditional SEPIC, by introduction of switched capacitors the rating and component sizing has been reduced and hence it can be working at comparatively high voltage without breaking the threshold limit of the capacitor. The closed loop controller design for the Modified SEPIC converter can be worked in both Constant current or Constant voltage , here the flow of power either in forward or reverse is controlled using a constant choosing a positive value will ensure the converter is working in forward direction and choosing negative value will make the converter work in negative direction. Another converter discussed in this thesis is Dual Active Bridge converter this isolated converter is in this topic design and analysis of single phase shift technique(SPS) for power flow in DAB converter is used the power transfer due to shifting of phases in between the primary and secondary coils of a transformer. The DAB converter is working in closed loop control system by appropriately implementing PI compensation technique and finding phase relation between Current and phase.

5.2 Future scope of work

In this thesis the use of bidirectional charger can be backed up by using a front end PFC converter which can make sure that the whole setup can withstand grid fluctuations, this is done with the help of a Voltage Source converter with LCL filter and the grid synchronization can be done using SOGI-PLL, we can also implement more robust control strategy instead if PI controller used in the following converter. Another converter discussed in this thesis is Dual Active Bridge converter this isolated converter is suitable for high voltage DC fast charging and can be further improved by using ZVS scheme for all the switches the DAB converter can be further explored with wide band Gap technologies to further increase the efficiency and decrease the overall sizing of component. Exploring more advanced control techniques to control the feedback mechanism by inclusion of techniques like Model predictive control (MPC) can be very insightful, there is also scope of muti port connection topology due to presence of transformer in DAB converter.

REFRENCES

[1] S. S. Williamson, Energy management strategies for electric and plug-in hybrid electric vehicles. Springer, 2013.

[2] a. Emadi and K. Rajashekara, "Power Electronics and Motor Drives in Electric, Hybrid Electric, and Plug-In Hybrid Electric Vehicles," IEEE Trans. Ind. Electron., vol. 55, no. 6, pp. 2237–2245, 2008.

[3] M. Yilmaz and P. T. Krein, "Review of charging power levels and infrastructure for plug-in electric and hybrid vehicles," 2012 IEEE Int. Electr. Veh. Conf. IEVC 2012, vol. 28, no. 5, pp. 2151–2169, 2012.

[4] Kavuri Poornesh1 , Kuzhivila Pannickottu Nivya2 , K. Sireesha3," A Comparative study on Electric Vehicle and Internal Combustion Engine Vehicles", Proceedings of the International Conference on Smart Electronics and Communication (ICOSEC 2020)

[5] H. Wang, S. Dusmez, and A. Khaligh, "Design and analysis of a full-bridge LLC-based PEV charger optimized for wide battery voltage range," IEEE Trans. Veh. Technol., vol. 63, no. 4, pp. 1603–1613, 2014.

[6] Huishuang Fan, Hongqi Ben and Jichao Ning, "Output voltage ripple reduction control strategy for three-phase combined PFC converter under grid voltage unbalance," in 22nd International Conference on Electrical Machines and Systems (ICEMS),2019.

[7] Rafael Pena-Alzola, Marco Andres Bianchi, Martin Ordonez, "Control Design of a PFC with Harmonic Mitigation Function for Small Hybrid AC/DC Buildings", IEEE Transactions on Power Electronics (Volume: 31, Issue: 9, September 2016).

[8] J. Gupta and B. Singh, "A Single Stage Bridgeless Isolated AC-DC Conversion System for Light Electric Vehicles Charging Application," IEEE Trans. Transp. Elect., Early Access, June 2022, doi: 10.1109/TTE.2022.3193314.

[9] Jinming Xu, Hao Qian, Yuan Hu, Shenyiyang bian, Shaojun Xie, "Overview of SOGI-Based Single-Phase Phase-Locked Loops for Grid Synchronization Under Complex Grid Conditions" IEEE Access 2021.

B. Whitaker, A. Barkley, Z. Cole, B. Passmore, D. Martin, T. R. McNutt, A. B. Lostetter, J. S. Lee, and K. Shiozaki, "A high-density, high efficiency, isolated on-board vehicle battery charger utilizing silicon carbide power

devices," IEEE Trans. Power Electron., vol. 29, no. 5, pp. 2606–2617, 2014

[10] A. Bocca and D. Baek, "Optimal Life-Cycle Costs of Batteries for Different Electric Cars," AEIT International Conference of Electrical and Electronic Technologies for Automotive (AEIT AUTOMOTIVE), pp. 1-6, 2020.

[11] T. Konjedic, L. Korosec, M. Truntic, C. Restrepo, M. Rodic, and M. Milanovic, "DCMbased Zero-Voltage Switching Control of a Bidirectional DC-DC Converter With Variable Switching Frequency," IEEE Trans. Power Electron., vol. 31, no. 4, pp. 3273–3288, 2015

[12] A. V. Mirtchev and E. C. Tatakis, "Design Methodology Based on Dual Control of a Resonant Dual Active Bridge Converter for Electric Vehicle Battery Charging," IEEE Trans. Veh. Tech., vol. 71, no. 3, pp. 2691-2705, March 2022.

[13] B. K. Padhi, S. N. Padhy and K. C. Bhuyan, "Controller design for reduced order model of SEPIC converter," *2016 International Conference on Signal Processing, Communication, Power and Embedded System (SCOPES)*.

[14] F. Jauch and J. Biela, "Generalized modeling and optimization of a bidirectional dual active bridge DC-DC converter including frequency variation," *2014 International Power Electronics Conference (IPEC-Hiroshima 2014 - ECCE ASIA)*, Hiroshima, Japan, 2014.

[15] D. Committee, I. Power, and E. Society, "IEEE Recommended Practice and Requirements for Harmonic Control in Electric Power Systems IEEE Power and Energy Society," vol. 2014, 2014.

[16] R. W. Erickson and D. Maksimovic, Fundamentals of power electronics. Springer Science & Business Media, 2007.

[17] Pratap Ranjan Mohanty, Anup Kumar Panda and Dhiman Das, "An Active PFC Boost Converter Topology for Power Factor Correction," Annual IEEE India Conference (INDICON), 2015

[18] Rahul Pandey and Bhim Singh, "A Power Factor Corrected Electric Vehicle Battery Charger Using Boost Converter 2018 8th IEEE India International Conference on Power Electronics (IICPE).

[19] João Paulo M. Figueiredo and Fernando L. Tofoli, "A Review of Single-Phase

[20] Murat Yilmaz and Philip T. Krein, “Review of Battery Charger Topologies, Charging Power Levels, and Infrastructure for Plug-In Electric and Hybrid Vehicles,” IEEE TRANSACTIONS ON POWER ELECTRONICS, VOL. 28, NO. 5, MAY 2013.

[21] wenjin Dai, and Ming Li, “Design of Single Phase Boost-PFC Converter With Fast voltage Regulator,” IEEE International Conference on Industrial Technology,2008.

[22] V. Randive and R. Wandhare, "Simplified State-Space Average Model and Control Strategy for the Dual Active Bridge Power Converter," *2020 IEEE 9th Power India International Conference (PIICON)*, Sonepat, India, 2020.

[23] Senthilkumar, R. and Justin Sunil Dhas, G. ‘Fractional Order Controller Design for SEPIC Converter Using Metaheuristic Algorithm’. 1 Jan. 2018

[24] S. Choudhury, “Average current mode controlled power factor correction converter using TMS320LF2407A,” Appl. Note SPRA902A. Texas Instruments, no. July, pp. 1–15, 2003

[25] H. Plesko, J. Biela, J. Luomi, and J. W. Kolar, “Novel concepts for integrating the electric drive and auxiliary DC-DC converter for hybrid vehicles,” IEEE Trans. Power Electron., vol. 23, no. 6, pp. 3025–3034, 2008

[26] S. Kim and F. S. Kang, “Multifunctional onboard battery charger for plug-in electric vehicles,” IEEE Trans. Ind. Electron., vol. 62, no. 6, pp. 3460–3472, 2015

[27] M. A. Khan, I. Husain, and Y. Sozer, “A Bi - directional DC - DC Converter with Overlapping Input and Output Voltage Ranges and Vehicle to Grid Energy Transfer Capability,” vol. 2, no. 3, pp. 507–516, 2014.

[28] R. Teodorescu, M. Liserre, and P. Rodriguez, "Grid Converters for Photovoltaic and Wind Power Systems," ed: John Wiley & Sons, Ltd., 2011

[29] H. Guan-Chyun and J. C. Hung, "Phase-locked loop techniques. A survey," Industrial Electronics, IEEE Transactions on, vol. 43, pp. 609-615, 1996

[30] M. Karimi-Ghartemani and M. R. Iravani, "A new phase-locked loop (PLL) system," in Circuits and Systems, 2001. MWSCAS 2001. Proceedings of the 44th IEEE 2001 Midwest Symposium on, 2001, pp. 421-424 vol.1

[31] S. Golestan, M. Monfared, F. D. Freijedo, and J. M. Guerrero, "Design and Tuning

of a Modified Power-Based PLL for Single-Phase Grid-Connected Power Conditioning Systems," Power Electronics, IEEE Transactions on, vol. 27, pp. 3639-3650, 2012

[32] A. zdemir, I. Yazici, and C. Vural, "Fast and robust software-based digital phase-locked loop for power electronics applications," Generation, Transmission & Distribution, IET, vol. 7, pp. 1435-1441, 2013

[33] A. Ohori, N. Hattori, and T. Funaki, "Phase-Locked Loop Using ComplexCoefficient Filters for Grid-Connected Inverter," Electrical Engineering in Japan, vol. 189, pp. 52-60, 2014

[34] M. M. Begovic, P. M. Djuric, S. Dunlap, and A. G. Phadke, "Frequency tracking in power networks in the presence of harmonics," Power Delivery, IEEE Transactions on, vol. 8, pp. 480-486, 1993.

[35] D. Nedeljkovic, J. Nastran, D. Voncina, and V. Ambrozic, "Synchronization of active power filter current reference to the network," Industrial Electronics, IEEE Transactions on, vol. 46, pp. 333-339, 1999

[36] R. Weidenbrug, F. P. Dawson, and R. Bonert, "New synchronization method for thyristor power converters to weak AC-systems," Industrial Electronics, IEEE Transactions on, vol. 40, pp. 505-511, 1993.

[37] R. W. Wall, "Simple methods for detecting zero crossing," in Industrial Electronics Society, 2003. IECON '03. The 29th Annual Conference of the IEEE, 2003, pp. 2477-2481 Vol.3

[38] P. Rodriguez, A. Luna, M. Ciobotaru, R. Teodorescu, and F. Blaabjerg, "Advanced Grid Synchronization System for Power Converters under Unbalanced and Distorted Operating Conditions," in IEEE Industrial Electronics, IECON 2006 - 32nd Annual Conference on, 2006, pp. 5173-5178.

[39] Gardner and F. M, "Phaselock Techniques," ed: John Wiley & Sons Inc, 1966.

[40] Utsav Sharma, and Bhim Singh, “An Onboard Charger for Light Electric Vehicles,” 2020 IEEE International Conference on Power Electronics, Drivesand Energy Systems (PEDES).

[42] Ionel “Dan” Jitaru, Nicolae Daniel Bolohan, “A High Efficiency 2KW DC-DC Converter for Automotive Application,” 2012 Twenty-Seventh Annual IEEE Applied Power Electronics Conference and Exposition (APEC).

[42] Chan-Song Lee, Jin-Beom Jeong, Baek-Haeng Lee, and Jin Hur, “Study on 1.5

kW Battery Chargers for Neighborhood Electric Vehicles", 2011 IEEE Vehicle Power and Propulsion Conference.

[43] Dingsihao Lyu, Thiago Batista Soeiro, and Pavol Bauer, "Impacts of Different Charging Strategies on the Electric Vehicle Battery Charger Circuit UsingPhase-Shift Full-Bridge Converter", 2021 IEEE 19th International PowerElectronics and Motion Control Conference (PEMC).

[44] Mohd Shahnawaz Khan, Shelas Sathyan, Harinaik Sugali,v and S S Chandra Bommagani," Design of On-Board Battery Charger using Interleaved Bridgeless Type PFC and Phase Shifted Full Bridge Converter",2020 IEEE International Students' Conference on Electrical, Electronics and Computer Science.

[45] Fariborz Musavi, Wilson Eberle, and William G. Dunford, "A High-Performance Single-Phase Bridgeless Interleaved PFC Converter for Plug-in Hybrid Electric Vehicle Battery Chargers",IEEE TRANSACTIONS ON INDUSTRY APPLICATIONS, VOL. 47, NO. 4, JULY/AUGUST 2011.